

Convergence analysis of the exponential matrix method for the solution of 3D equilibrium equations for free vibration analysis of plates and shells

*Original*

Convergence analysis of the exponential matrix method for the solution of 3D equilibrium equations for free vibration analysis of plates and shells / Brischetto, Salvatore. - In: COMPOSITES. PART B, ENGINEERING. - ISSN 1359-8368. - 98:(2016), pp. 453-471. [10.1016/j.compositesb.2016.05.047]

*Availability:*

This version is available at: 11583/2643239 since: 2020-06-04T00:06:22Z

*Publisher:*

Elsevier

*Published*

DOI:10.1016/j.compositesb.2016.05.047

*Terms of use:*

This article is made available under terms and conditions as specified in the corresponding bibliographic description in the repository

*Publisher copyright*

(Article begins on next page)

# Convergence analysis of the exponential matrix method for the solution of 3D equilibrium equations for free vibration analysis of plates and shells

Salvatore Brischetto\*

## Abstract

*The three-dimensional equilibrium dynamic equations written in general curvilinear orthogonal coordinates allow the free vibration analysis of one-layered and multilayered plates and shells. The system of second order differential equations is transformed into a system of first order differential equations. Such a system is exactly solved using the exponential matrix method which is calculated by means of an expansion with a very fast convergence ratio. In the case of plate geometries, the differential equations have constant coefficients. The differential equations have variable coefficients in the case of shell geometries because of the curvature terms which depend on the thickness coordinate  $z$ . In shell cases, several mathematical layers must be introduced to approximate the curvature terms and to obtain differential equations with constant coefficients. The present work investigates the convergence of the proposed method related to the order  $N$  used for the expansion of the exponential matrix and to the number of mathematical layers  $M$  used for the solution of shell equations. Both  $N$  and  $M$  values are analyzed for different geometries, thickness ratios, materials, lamination sequences, imposed half-wave numbers, frequency orders and vibration modes.*

**Keywords:** plates; shells; free vibrations; 3D elasticity solution; exact method; exponential matrix method; convergence study; mathematical layers.

## 1 Introduction

Plates and shells are fundamental elements for the analysis of one-layered and multilayered structures embedding homogeneous and composite layers. These two-dimensional (2D) elements need an accurate validation to be used with confidence in several engineering applications [1], [2]. Three-dimensional (3D) exact solutions can be used to validate and check 2D models. Moreover, 3D solutions give further details about three-dimensional behavior and complicating effects introduced by multilayered configurations, e.g., the coupling between shear and axial strains, the zigzag form of displacements through the thickness and interlaminar continuity problems [3], [4]. In the literature, exact three-dimensional solutions do not give a general overview of plate and shell elements because they analyze the various geometries separately. The proposed 3D general formulation in orthogonal curvilinear coordinates for the equations of motion is valid for multilayered square and rectangular plates, cylindrical shell panels, spherical shell panels and cylinders. The present 3D model exactly solves the equations of motion

---

\*Corresponding author: Salvatore Brischetto, Department of Mechanical and Aerospace Engineering, Politecnico di Torino, corso Duca degli Abruzzi, 24, 10129 Torino, ITALY. tel: +39.011.090.6813, fax: +39.011.090.6899, e.mail: salvatore.brischetto@polito.it.

in general curvilinear orthogonal coordinates including an exact geometry for shell structures without simplifications. The method is based on a layer-wise approach which imposes the continuity of displacements and transverse shear/normal stresses at the interfaces between layers embedded in the multilayered plates and shells. The exponential matrix method [5]- [8] is used to solve the differential equations which have variable coefficients in the case of shell geometries because of the curvature terms. In this case, several mathematical layers are introduced to consider constant curvature terms in the equilibrium equations. Details about the proposed 3D model can be found in past author's works [9]- [17]. Similar approaches have been used in [18] for the three-dimensional analysis of plates in rectilinear orthogonal coordinates and in [19] for an exact, three-dimensional, free vibration analysis of angle-ply laminated cylinders in cylindrical coordinates. The equations of motion written in orthogonal curvilinear coordinates can be considered as a general form of the equations of motions written in rectilinear orthogonal coordinates [18] and in cylindrical coordinates [19]. The present equations allow general exact solutions for multilayered plate and shell geometries.

The revision of the literature about three-dimensional analysis of shells and plates demonstrates that there is a variety of interesting works concerning plate or shell geometry. They include static and dynamic analysis, functionally graded, composite and piezoelectric materials, displacement and mixed models. However, the present 3D model constitutes a breakthrough because it gives a general formulation for all the geometries (square and rectangular plates, cylindrical and spherical shell panels, and cylindrical closed shells).

The most relevant works about three-dimensional shell analysis are summarized in the following part. Chen et al. [20] analyzed the exact coupled free vibrations of a transversely isotropic cylindrical shell embedded in an elastic medium. Fan and Zhang [21] proposed the exact solutions for static, dynamic and buckling analysis of thick laminated cylindrical shells using the Cayley-Hamilton theorem. Gasemzadeh et al. [22] studied the exact three-dimensional free vibrations of cylindrical shells. The free vibrations of simply-supported cross-ply cylindrical and doubly-curved laminates were proposed in [23]. Sharma et al. [24] showed the three-dimensional free vibrations of a homogenous isotropic, viscothermoelastic hollow sphere with surfaces subjected to stress-free, thermally insulated or isothermal boundary conditions. A similar procedure was used for the exact three-dimensional vibration analysis of a trans-radially isotropic, thermoelastic solid sphere [25]. Soldatos and Ye [19] proposed exact, three-dimensional, free vibration analysis of angle-ply laminated cylinders. Armenakas et al. [26] developed a self-contained study of plane harmonic wave propagation along a hollow circular cylinder using the three-dimensional theory of elasticity. A thorough comparison between frequencies obtained from a refined two-dimensional analysis, a shear deformation theory, the Flügge theory and an exact elasticity analysis were proposed in [27]. Some details about the Flügge classical thin shell theory applied to the free vibrations of cylindrical shells with elastic boundary conditions were given in [28]. Exact elasticity solutions were extended to functionally graded cylindrical shells in [29]. The three-dimensional linear elastodynamics equations were solved using suitable displacement functions that identically satisfy the boundary conditions. Loy and Lam [30] developed a layer wise approach for the vibration of thick circular cylindrical shells using the three-dimensional theory of elasticity. Wang et al. [31] investigated the free vibrations of magneto-electro-elastic cylindrical panels based on the three-dimensional theory. Further results about numerical three-dimensional analysis of shells were shown by Efraim and Eisenberger [32] for the dynamic stiffness matrix method, and by Kang and Leissa [33] and Liew et al. [34] for the three-dimensional Ritz method for vibration of spherical shells.

Equilibrium equations for the three-dimensional analysis of plates are usually simpler than those for shells and they do not allow the analysis of curved structures. Aimmanee and Batra [35] developed an analytical solution for free vibrations of a simply supported rectangular plate made of an incompressible homogeneous linear elastic isotropic material. A similar approach for in-plane modes of a simply supported rectangular plate were proposed in [36]. A three-dimensional linear elastic, small deformation theory obtained by the direct method was developed for the free vibration of simply sup-

ported, homogeneous, isotropic, thick rectangular plates in [37]. A similar method was used in [38] for the flexure of simply supported homogeneous, isotropic, thick rectangular plates under arbitrary loadings. Comparisons between two-dimensional models and an exact three-dimensional solution for the free vibrations of a simply supported rectangular orthotropic thick plate were shown in [39]. On the basis of three-dimensional elasticity, Ye [40] developed a free vibration analysis of cross-ply laminated rectangular plates with clamped boundaries. Comparisons between 2D-displacement-based-models and the linear three-dimensional exact elasticity results were proposed in [18] for natural frequencies, displacement and stress quantities of multilayered plates. Exact three-dimensional elasticity theory was investigated in [41] for isosceles triangular plates by means of a global three-dimensional Ritz formulation. The three-dimensional elastic free vibration analysis of a circular plate was analyzed in [42] by means of the Ritz method using a set of orthogonal polynomial series for the spatial displacement approximations. High frequency vibration analyses are indispensable in a variety of engineering designs. Zhao et al. [43] introduced a novel computational approach (the discrete singular convolution algorithm) for high frequency vibration analysis of plate structures. A completely independent approach, based on the Levy method, was employed to provide exact solutions to validated the proposed method. Further works about the analysis of high-frequency vibrations of structures are given in [44] and [45]. Three-dimensional elasticity theory and the Ritz method was applied to derive the eigenvalue equation in [45]. Xing and Liu [46] proposed the separation of variables to solve the Hamiltonian dual form of eigenvalue problem for transverse free vibrations of thin plates. A formulation for the natural modes in closed form was also performed. The extension of 3D exact analysis to functionally graded plates was proposed in [47]- [49]. The extension of three-dimensional solutions to piezoelectric multilayered plates was given in [50]- [55].

The proposed three-dimensional equilibrium equations are written in general orthogonal curvilinear coordinates and they can be used for the free vibration analysis of plates, cylinders and cylindrical/spherical shell panels. The solution is written in exact/close form considering simply supported structures and harmonic form for displacement components. The system of second order partial differential equations is reduced to a system of first order partial differential equations redoubling the variables. Resulting differential equations are solved using the exponential matrix method. The exponential matrix is developed in the thickness direction with an opportune order  $N$ . The shell equilibrium equations have variable coefficients because of the parametric coefficients which include curvatures and the thickness coordinate  $z$ . Such equations are simpler in the plate cases where they show constant coefficients. In the case of a system of partial differential equations with variable coefficients (shells case), several mathematical layers  $M$ , to approximate the curvature terms, are introduced to solve the system. The present paper proposes a convergence analysis for the order  $N$  used in the exponential matrix and for the number of mathematical layers  $M$  in the case of plates and shells with different materials, thickness ratios, geometries and lamination sequences. This convergence study is also proposed for several frequency orders, half-wave numbers and vibration modes. In the works where this method was accurately described [5]- [8] or used [9]- [19], this systematic and thorough study was not contemplated. The proposed convergence analysis for both parameters  $M$  and  $N$  should be useful to optimise the 3D model in terms of residual error and convergence speed. In general, the expansion of the exponential matrix is stable and has a very fast convergence. The use of mathematical layers  $M$  needs a higher attention.

## 2 Three-dimensional equilibrium equations for shells

The three differential equations of equilibrium for the free vibration analysis of multilayered spherical shells made of  $N_L$  layers with constant radii of curvature  $R_\alpha$  and  $R_\beta$  are:

$$H_\beta \frac{\partial \sigma_{\alpha\alpha}^k}{\partial \alpha} + H_\alpha \frac{\partial \sigma_{\alpha\beta}^k}{\partial \beta} + H_\alpha H_\beta \frac{\partial \sigma_{\alpha z}^k}{\partial z} + \left( \frac{2H_\beta}{R_\alpha} + \frac{H_\alpha}{R_\beta} \right) \sigma_{\alpha z}^k = \rho^k H_\alpha H_\beta \ddot{u}^k, \quad (1)$$

$$H_\beta \frac{\partial \sigma_{\alpha\beta}^k}{\partial \alpha} + H_\alpha \frac{\partial \sigma_{\beta\beta}^k}{\partial \beta} + H_\alpha H_\beta \frac{\partial \sigma_{\beta z}^k}{\partial z} + \left( \frac{2H_\alpha}{R_\beta} + \frac{H_\beta}{R_\alpha} \right) \sigma_{\beta z}^k = \rho^k H_\alpha H_\beta \ddot{v}^k, \quad (2)$$

$$H_\beta \frac{\partial \sigma_{\alpha z}^k}{\partial \alpha} + H_\alpha \frac{\partial \sigma_{\beta z}^k}{\partial \beta} + H_\alpha H_\beta \frac{\partial \sigma_{zz}^k}{\partial z} - \frac{H_\beta}{R_\alpha} \sigma_{\alpha\alpha}^k - \frac{H_\alpha}{R_\beta} \sigma_{\beta\beta}^k + \left( \frac{H_\beta}{R_\alpha} + \frac{H_\alpha}{R_\beta} \right) \sigma_{zz}^k = \rho^k H_\alpha H_\beta \ddot{w}^k, \quad (3)$$

the most general form for variable radii of curvature can be found in [2] and [56].  $\rho^k$  is the mass density,  $(\sigma_{\alpha\alpha}^k, \sigma_{\beta\beta}^k, \sigma_{zz}^k, \sigma_{\beta z}^k, \sigma_{\alpha z}^k, \sigma_{\alpha\beta}^k)$  are the six stress components and  $\ddot{u}^k, \ddot{v}^k$  and  $\ddot{w}^k$  indicate the second temporal derivative of the three displacement components.  $k$  indicates the general layer. Symbol  $\partial$  indicates the partial derivatives.  $R_\alpha$  and  $R_\beta$  are referred to the mid-surface  $\Omega_0$  of the whole multilayered shell (details about notations and reference system for shells are shown in Figure 1). Parametric coefficients  $H_\alpha$  and  $H_\beta$  continuously vary through the thickness of the whole multilayered shell and depend on the thickness coordinate:

$$H_\alpha = \left( 1 + \frac{z}{R_\alpha} \right) = \left( 1 + \frac{\tilde{z} - h/2}{R_\alpha} \right), \quad H_\beta = \left( 1 + \frac{z}{R_\beta} \right) = \left( 1 + \frac{\tilde{z} - h/2}{R_\beta} \right), \quad H_z = 1, \quad (4)$$

$H_\alpha$  and  $H_\beta$  depend on the  $z$  or  $\tilde{z}$  coordinate (see Figure 2 for further details about the coordinate systems). Geometry and the reference system are indicated in Figure 1 where curvilinear orthogonal coordinates  $(\alpha, \beta, z)$  are shown. Displacement components are indicated as  $u, v$ , and  $w$  in  $\alpha, \beta$  and  $z$  directions, respectively.

The geometrical relations in orthogonal curvilinear coordinates which link strains with displacements in the case of three-dimensional theory of elasticity were shown in [56] and [57] for the generic  $k$  layer of the multilayered shell. In the present paper, the attention is focused to shells with constant radii of curvature (e.g., cylindrical and spherical geometries). The geometrical relations for shells with constant radii of curvature are:

$$\epsilon_{\alpha\alpha}^k = \frac{1}{H_\alpha} \frac{\partial u^k}{\partial \alpha} + \frac{w^k}{H_\alpha R_\alpha}, \quad (5)$$

$$\epsilon_{\beta\beta}^k = \frac{1}{H_\beta} \frac{\partial v^k}{\partial \beta} + \frac{w^k}{H_\beta R_\beta}, \quad (6)$$

$$\epsilon_{zz}^k = \frac{\partial w^k}{\partial z}, \quad (7)$$

$$\gamma_{\beta z}^k = \frac{1}{H_\beta} \frac{\partial w^k}{\partial \beta} + \frac{\partial v^k}{\partial z} - \frac{v^k}{H_\beta R_\beta}, \quad (8)$$

$$\gamma_{\alpha z}^k = \frac{1}{H_\alpha} \frac{\partial w^k}{\partial \alpha} + \frac{\partial u^k}{\partial z} - \frac{u^k}{H_\alpha R_\alpha}, \quad (9)$$

$$\gamma_{\alpha\beta}^k = \frac{1}{H_\alpha} \frac{\partial v^k}{\partial \alpha} + \frac{1}{H_\beta} \frac{\partial u^k}{\partial \beta}. \quad (10)$$

These general relations for spherical shells degenerate into geometrical relations for cylindrical shells when  $R_\alpha$  or  $R_\beta$  is infinite (with  $H_\alpha$  or  $H_\beta$  equals one), and they degenerate into geometrical relations for plates when both  $R_\alpha$  and  $R_\beta$  are infinite (with  $H_\alpha=H_\beta=1$ ).

The three-dimensional linear elastic constitutive equations in orthogonal curvilinear coordinates ( $\alpha$ ,  $\beta$ ,  $z$ ) and in matrix form for orthotropic material in the structural reference system is here given for a generic  $k$  layer of the multilayered structure:

$$\boldsymbol{\sigma}^k = \mathbf{C}^k \boldsymbol{\epsilon}^k, \quad (11)$$

the  $6 \times 1$  vector of stress components  $\boldsymbol{\sigma}^k = \{\sigma_{\alpha\alpha}^k, \sigma_{\beta\beta}^k, \sigma_{zz}^k, \sigma_{\beta z}^k, \sigma_{\alpha z}^k, \sigma_{\alpha\beta}^k\}^T$  is linked with the the  $6 \times 1$  vector of strain components  $\boldsymbol{\epsilon}^k = \{\epsilon_{\alpha\alpha}^k, \epsilon_{\beta\beta}^k, \epsilon_{zz}^k, \gamma_{\beta z}^k, \gamma_{\alpha z}^k, \gamma_{\alpha\beta}^k\}^T$  by means of the  $6 \times 6$  matrix  $\mathbf{C}^k$  containing the elastic coefficients. Details about this matrix are described in [3] and [4]. A closed form solution of differential equations of equilibrium for shells are obtained imposing coefficients  $C_{16}^k$ ,  $C_{26}^k$ ,  $C_{36}^k$  and  $C_{45}^k$  equal to zero (this means orthotropic angle  $\theta$  equals  $0^\circ$  or  $90^\circ$ ).

Geometrical equations (5)-(10) and constitutive equations (11) are included in eqs.(1)-(3) in order to obtain a displacement form of the equilibrium relations. The differential equations of equilibrium for a generic  $k$  layer in displacement form are:

$$\begin{aligned} & \left(-\frac{H_\beta C_{55}^k}{H_\alpha R_\alpha^2} - \frac{C_{55}^k}{R_\alpha R_\beta}\right)u^k + \left(\frac{C_{55}^k H_\beta}{R_\alpha} + \frac{C_{55}^k H_\alpha}{R_\beta}\right)u_{,z}^k + \left(\frac{C_{11}^k H_\beta}{H_\alpha}\right)u_{,\alpha\alpha}^k + \left(\frac{C_{66}^k H_\alpha}{H_\beta}\right)u_{,\beta\beta}^k + (C_{55}^k H_\alpha H_\beta)u_{,zz}^k + \\ & (C_{12}^k + C_{66}^k)v_{,\alpha\beta}^k + \left(\frac{C_{11}^k H_\beta}{H_\alpha R_\alpha} + \frac{C_{12}^k}{R_\beta} + \frac{C_{55}^k H_\beta}{H_\alpha R_\alpha} + \frac{C_{55}^k}{R_\beta}\right)w_{,\alpha}^k + (C_{13}^k H_\beta + C_{55}^k H_\beta)w_{,\alpha z}^k = \rho^k H_\alpha H_\beta \ddot{u}^k, \quad (12) \end{aligned}$$

$$\begin{aligned} & \left(-\frac{H_\alpha C_{44}^k}{H_\beta R_\beta^2} - \frac{C_{44}^k}{R_\alpha R_\beta}\right)v^k + \left(\frac{C_{44}^k H_\alpha}{R_\beta} + \frac{C_{44}^k H_\beta}{R_\alpha}\right)v_{,z}^k + \left(\frac{C_{66}^k H_\beta}{H_\alpha}\right)v_{,\alpha\alpha}^k + \left(\frac{C_{22}^k H_\alpha}{H_\beta}\right)v_{,\beta\beta}^k + (C_{44}^k H_\alpha H_\beta)v_{,zz}^k + \\ & (C_{12}^k + C_{66}^k)u_{,\alpha\beta}^k + \left(\frac{C_{44}^k H_\alpha}{H_\beta R_\beta} + \frac{C_{44}^k}{R_\alpha} + \frac{C_{22}^k H_\alpha}{H_\beta R_\beta} + \frac{C_{12}^k}{R_\alpha}\right)w_{,\beta}^k + (C_{44}^k H_\alpha + C_{23}^k H_\alpha)w_{,\beta z}^k = \rho^k H_\alpha H_\beta \ddot{v}^k, \quad (13) \end{aligned}$$

$$\begin{aligned} & \left(\frac{C_{13}^k}{R_\alpha R_\beta} + \frac{C_{23}^k}{R_\alpha R_\beta} - \frac{C_{11}^k H_\beta}{H_\alpha R_\alpha^2} - \frac{2C_{12}^k}{R_\alpha R_\beta} - \frac{C_{22}^k H_\alpha}{H_\beta R_\beta^2}\right)w^k + \left(-\frac{C_{55}^k H_\beta}{H_\alpha R_\alpha} + \frac{C_{13}^k}{R_\beta} - \frac{C_{11}^k H_\beta}{H_\alpha R_\alpha} - \frac{C_{12}^k}{R_\beta}\right)u_{,\alpha}^k + \\ & \left(-\frac{C_{44}^k H_\alpha}{H_\beta R_\beta} + \frac{C_{23}^k}{R_\alpha} - \frac{C_{22}^k H_\alpha}{H_\beta R_\beta} - \frac{C_{12}^k}{R_\alpha}\right)v_{,\beta}^k + \left(\frac{C_{33}^k H_\beta}{R_\alpha} + \frac{C_{33}^k H_\alpha}{R_\beta}\right)w_{,z}^k + (C_{55}^k H_\beta + C_{13}^k H_\beta)u_{,\alpha z}^k + \\ & (C_{44}^k H_\alpha + C_{23}^k H_\alpha)v_{,\beta z}^k + (C_{55}^k \frac{H_\beta}{H_\alpha})w_{,\alpha\alpha}^k + (C_{44}^k \frac{H_\alpha}{H_\beta})w_{,\beta\beta}^k + (C_{33}^k H_\alpha H_\beta)w_{,zz}^k = \rho^k H_\alpha H_\beta \ddot{w}^k. \quad (14) \end{aligned}$$

$H_\alpha$  and  $H_\beta$  are calculated through the thickness of the whole multilayered shell by means of eqs.(4). Equilibrium equations (12)-(14) are for spherical shell panels, they automatically degenerate into equilibrium equations for cylindrical closed/open shell panels when  $R_\alpha$  or  $R_\beta$  is infinite ( $H_\alpha$  or  $H_\beta$  equals one) and into equilibrium equations for plates when both  $R_\alpha$  and  $R_\beta$  are infinite ( $H_\alpha$  and  $H_\beta$  equal one). This formulation allows a unique and general formulation for any geometry. Partial derivatives  $\frac{\partial}{\partial\alpha}$ ,  $\frac{\partial}{\partial\beta}$  and  $\frac{\partial}{\partial z}$  are indicated with subscripts  $_{,\alpha}$ ,  $_{,\beta}$  and  $_{,z}$ .

### 3 Exact solution and exponential matrix method

The closed form of eqs.(12)-(14) is developed for simply supported shells and plates. The harmonic form of the three displacement components is:

$$u^k(\alpha, \beta, z, t) = U^k(z)e^{i\omega t} \cos(\bar{\alpha}\alpha) \sin(\bar{\beta}\beta), \quad (15)$$

$$v^k(\alpha, \beta, z, t) = V^k(z)e^{i\omega t} \sin(\bar{\alpha}\alpha) \cos(\bar{\beta}\beta), \quad (16)$$

$$w^k(\alpha, \beta, z, t) = W^k(z)e^{i\omega t} \sin(\bar{\alpha}\alpha) \sin(\bar{\beta}\beta), \quad (17)$$

$U^k$ ,  $V^k$  and  $W^k$  are the displacement amplitudes in  $\alpha$ ,  $\beta$  and  $z$  directions, respectively.  $\omega=2\pi f$  is the circular frequency where  $f$  is the frequency value,  $t$  is the time.  $i$  is the coefficient of the imaginary

unit. In coefficients  $\bar{\alpha} = \frac{m\pi}{a}$  and  $\bar{\beta} = \frac{n\pi}{b}$ , m and n are the half-wave numbers and a and b are the shell dimensions in  $\alpha$  and  $\beta$  directions, respectively, calculated in the mid-surface  $\Omega_0$ .

Eqs.(15)-(17) are substituted in eqs.(12)-(14) to obtain the following system:

$$\begin{aligned} & \left( -\frac{C_{55}^j H_\beta}{H_\alpha R_\alpha^2} - \frac{C_{55}^j}{R_\alpha R_\beta} - \bar{\alpha}^2 \frac{C_{11}^j H_\beta}{H_\alpha} - \bar{\beta}^2 \frac{C_{66}^j H_\alpha}{H_\beta} + \rho^j H_\alpha H_\beta \omega^2 \right) U^j + (-\bar{\alpha} \bar{\beta} C_{12}^j - \bar{\alpha} \bar{\beta} C_{66}^j) V^j + \\ & \left( \bar{\alpha} \frac{C_{11}^j H_\beta}{H_\alpha R_\alpha} + \bar{\alpha} \frac{C_{12}^j}{R_\beta} + \bar{\alpha} \frac{C_{55}^j H_\beta}{H_\alpha R_\alpha} + \bar{\alpha} \frac{C_{55}^j}{R_\beta} \right) W^j + \left( \frac{C_{55}^j H_\beta}{R_\alpha} + \frac{C_{55}^j H_\alpha}{R_\beta} \right) U_{,z}^j + (\bar{\alpha} C_{13}^j H_\beta + \bar{\alpha} C_{55}^j H_\beta) W_{,z}^j + \end{aligned} \quad (18)$$

$$(C_{55}^j H_\alpha H_\beta) U_{,zz}^j = 0 ,$$

$$\begin{aligned} & (-\bar{\alpha} \bar{\beta} C_{66}^j - \bar{\alpha} \bar{\beta} C_{12}^j) U^j + \left( -\frac{C_{44}^j H_\alpha}{H_\beta R_\beta^2} - \frac{C_{44}^j}{R_\alpha R_\beta} - \bar{\alpha}^2 \frac{C_{66}^j H_\beta}{H_\alpha} - \bar{\beta}^2 \frac{C_{22}^j H_\alpha}{H_\beta} + \rho^j H_\alpha H_\beta \omega^2 \right) V^j + \\ & \left( \bar{\beta} \frac{C_{44}^j H_\alpha}{H_\beta R_\beta} + \bar{\beta} \frac{C_{44}^j}{R_\alpha} + \bar{\beta} \frac{C_{22}^j H_\alpha}{H_\beta R_\beta} + \bar{\beta} \frac{C_{12}^j}{R_\alpha} \right) W^j + \left( \frac{C_{44}^j H_\alpha}{R_\beta} + \frac{C_{44}^j H_\beta}{R_\alpha} \right) V_{,z}^j + (\bar{\beta} C_{44}^j H_\alpha + \bar{\beta} C_{23}^j H_\alpha) W_{,z}^j + \end{aligned} \quad (19)$$

$$(C_{44}^j H_\alpha H_\beta) V_{,zz}^j = 0 ,$$

$$\begin{aligned} & \left( \bar{\alpha} \frac{C_{55}^j H_\beta}{H_\alpha R_\alpha} - \bar{\alpha} \frac{C_{13}^j}{R_\beta} + \bar{\alpha} \frac{C_{11}^j H_\beta}{H_\alpha R_\alpha} + \bar{\alpha} \frac{C_{12}^j}{R_\beta} \right) U^j + \left( \bar{\beta} \frac{C_{44}^j H_\alpha}{H_\beta R_\beta} - \bar{\beta} \frac{C_{23}^j}{R_\alpha} + \bar{\beta} \frac{C_{22}^j H_\alpha}{H_\beta R_\beta} + \bar{\beta} \frac{C_{12}^j}{R_\alpha} \right) V^j + \left( \frac{C_{13}^j}{R_\alpha R_\beta} + \right. \\ & \left. \frac{C_{23}^j}{R_\alpha R_\beta} - \frac{C_{11}^j H_\beta}{H_\alpha R_\alpha^2} - \frac{2C_{12}^j}{R_\alpha R_\beta} - \frac{C_{22}^j H_\alpha}{H_\beta R_\beta^2} - \bar{\alpha}^2 \frac{C_{55}^j H_\beta}{H_\alpha} - \bar{\beta}^2 \frac{C_{44}^j H_\alpha}{H_\beta} + \rho^j H_\alpha H_\beta \omega^2 \right) W^j + (-\bar{\alpha} C_{55}^j H_\beta - \end{aligned} \quad (20)$$

$$\bar{\alpha} C_{13}^j H_\beta) U_{,z}^j + (-\bar{\beta} C_{44}^j H_\alpha - \bar{\beta} C_{23}^j H_\alpha) V_{,z}^j + \left( \frac{C_{33}^j H_\beta}{R_\alpha} + \frac{C_{33}^j H_\alpha}{R_\beta} \right) W_{,z}^j + (C_{33}^j H_\alpha H_\beta) W_{,zz}^j = 0 .$$

Coefficients in eqs.(18)-(20), which multiply displacements and their derivatives in z, are variable in the case of shell geometry because parametric coefficients  $H_\alpha$  and  $H_\beta$  depend on the z coordinate (see Figure 2).  $H_\alpha=H_\beta=1$  in the case of plate geometry (both radii of curvature  $R_\alpha$  and  $R_\beta$  are infinite), and eqs.(18)-(20) have constant coefficients and they can be directly solved via the exponential matrix method. For shell geometries, several l mathematical layers are included in each k physical layer in order to calculate  $H_\alpha$  and  $H_\beta$ . Coefficients are constant in the l layer because they are evaluated with  $R_\alpha$ ,  $R_\beta$ ,  $\bar{\alpha}$  and  $\bar{\beta}$  considered in the mid-surface  $\Omega_0$  of the whole shell, and with  $H_\alpha$  and  $H_\beta$  considered in the middle of each l layer. In the present paper, each k physical layer of the multilayered structures is divided in l mathematical layers. The total index for both mathematical and physical layers is  $j=k \times l$ . Examples of introduction of j mathematical layers in shell geometries are given in Figures 3, 4 and 5 for a one-layered shell (1 physical layer,  $N_L=1$ ), a three-layered shell (3 physical layers,  $N_L=3$ ) and a five-layered shell (5 physical layers,  $N_L=5$ ), respectively, are divided in  $j=M=10$  mathematical layers.

The system of eqs.(18)-(20) are developed in a compact form by introducing coefficients  $A_s^j$  (with s from 1 to 19) for each block in parentheses which multiplies displacement components or their derivatives:

$$A_1^j U^j + A_2^j V^j + A_3^j W^j + A_4^j U_{,z}^j + A_5^j W_{,z}^j + A_6^j U_{,zz}^j = 0 , \quad (21)$$

$$A_7^j U^j + A_8^j V^j + A_9^j W^j + A_{10}^j V_{,z}^j + A_{11}^j W_{,z}^j + A_{12}^j V_{,zz}^j = 0 , \quad (22)$$

$$A_{13}^j U^j + A_{14}^j V^j + A_{15}^j W^j + A_{16}^j U_{,z}^j + A_{17}^j V_{,z}^j + A_{18}^j W_{,z}^j + A_{19}^j W_{,zz}^j = 0 . \quad (23)$$

The eqs.(21)-(23) are a system of three second order differential equations. These equations have been developed for spherical shell panels with constant radii of curvature but they automatically degenerate into equations for cylindrical shells and plates.

The system of second order differential equations is reduced to a system of first order differential equations using the method described in [5] and [6] where the number of variables has been redoubled.

Details about this methodology can be found in [10] and [11]. This method allows to write:

$$\begin{bmatrix} A_6^j & 0 & 0 & 0 & 0 & 0 \\ 0 & A_{12}^j & 0 & 0 & 0 & 0 \\ 0 & 0 & A_{19}^j & 0 & 0 & 0 \\ 0 & 0 & 0 & A_6^j & 0 & 0 \\ 0 & 0 & 0 & 0 & A_{12}^j & 0 \\ 0 & 0 & 0 & 0 & 0 & A_{19}^j \end{bmatrix} \begin{bmatrix} U^j \\ V^j \\ W^j \\ U^{j'} \\ V^{j'} \\ W^{j'} \end{bmatrix}' = \begin{bmatrix} 0 & 0 & 0 & A_6^j & 0 & 0 \\ 0 & 0 & 0 & 0 & A_{12}^j & 0 \\ 0 & 0 & 0 & 0 & 0 & A_{19}^j \\ -A_1^j & -A_2^j & -A_3^j & -A_4^j & 0 & -A_5^j \\ -A_7^j & -A_8^j & -A_9^j & 0 & -A_{10}^j & -A_{11}^j \\ -A_{13}^j & -A_{14}^j & -A_{15}^j & -A_{16}^j & -A_{17}^j & -A_{18}^j \end{bmatrix} \begin{bmatrix} U^j \\ V^j \\ W^j \\ U^{j'} \\ V^{j'} \\ W^{j'} \end{bmatrix}. \quad (24)$$

Eq.(24) can be written in a compact form for a generic j layer:

$$\mathbf{D}^j \frac{\partial \mathbf{U}^j}{\partial \tilde{z}} = \mathbf{A}^j \mathbf{U}^j, \quad (25)$$

where  $\frac{\partial \mathbf{U}^j}{\partial \tilde{z}} = \mathbf{U}^{j'}$  and  $\mathbf{U}^j = [U^j \ V^j \ W^j \ U^{j'} \ V^{j'} \ W^{j'}]$ . The eq.(25) can be developed as:

$$\mathbf{D}^j \mathbf{U}^{j'} = \mathbf{A}^j \mathbf{U}^j, \quad (26)$$

$$\mathbf{U}^{j'} = \mathbf{D}^{j-1} \mathbf{A}^j \mathbf{U}^j, \quad (27)$$

$$\mathbf{U}^{j'} = \mathbf{A}^{j*} \mathbf{U}^j, \quad (28)$$

with  $\mathbf{A}^{j*} = \mathbf{D}^{j-1} \mathbf{A}^j$ .

The solution of eq.(28), in accordance to [6], [7], is:

$$\mathbf{U}^j(\tilde{z}^j) = \exp(\mathbf{A}^{j*} \tilde{z}^j) \mathbf{U}^j(0) \quad \text{with} \quad \tilde{z}^j \in [0, h^j], \quad (29)$$

where  $\tilde{z}^j$  is the thickness coordinate of each layer from 0 at the bottom to  $h^j$  at the top (see Figure 2). The exponential matrix for each j mathematical layer, with constant coefficients  $A_s^j$ , is calculated with  $\tilde{z}^j = h^j$ :

$$\mathbf{A}^{j**} = \exp(\mathbf{A}^{j*} h^j) = \mathbf{I} + \mathbf{A}^{j*} h^j + \frac{\mathbf{A}^{j*2}}{2!} h^{j2} + \frac{\mathbf{A}^{j*3}}{3!} h^{j3} + \dots + \frac{\mathbf{A}^{j*N}}{N!} h^{jN}, \quad (30)$$

$\mathbf{I}$  is the  $6 \times 6$  identity matrix. The proposed expansion has a fast convergence ratio as indicated in [8] and it is not time consuming from the computational point of view.

M-1 transfer matrices  $\mathbf{T}^{j-1,j}$  must be calculated using for each interface the following conditions for interlaminar continuity of displacements and transverse shear/normal stresses:

$$u_b^j = u_t^{j-1}, \quad v_b^j = v_t^{j-1}, \quad w_b^j = w_t^{j-1}, \quad (31)$$

$$\sigma_{zzb}^j = \sigma_{zzt}^{j-1}, \quad \sigma_{\alpha zb}^j = \sigma_{\alpha zt}^{j-1}, \quad \sigma_{\beta zb}^j = \sigma_{\beta zt}^{j-1}, \quad (32)$$

where displacements and transverse shear/normal stresses at the bottom (b) of the j layer must be equal to displacements and transverse shear/normal stresses at the top (t) of the (j-1) layer.

The structures are considered as simply supported and free stresses at the top and at the bottom of the whole multilayered shell:

$$\sigma_{zz} = \sigma_{\alpha z} = \sigma_{\beta z} = 0 \quad \text{for} \quad z = -h/2, +h/2 \quad \text{or} \quad \tilde{z} = 0, h, \quad (33)$$

$$w = v = 0, \quad \sigma_{\alpha\alpha} = 0 \quad \text{for} \quad \alpha = 0, a, \quad (34)$$

$$w = u = 0, \quad \sigma_{\beta\beta} = 0 \quad \text{for} \quad \beta = 0, b, \quad (35)$$

The use of solution proposed in eq.(30) and the introduction of the conditions written in eqs.(31)-(32) and eqs.(33)-(35) give the following compact form for final system:

$$\mathbf{E} \ \mathbf{U}_1(0) = \mathbf{0} \ . \quad (36)$$



All the details about the steps, omitted in this paper, to obtain the final equation (36), can be found in past author's works [9]- [11]. Matrix  $\mathbf{E}$  has always  $6 \times 6$  dimension, independently from the employed number of physical and mathematical layers M and even if the method uses a layer-wise approach. Each term in the matrix  $\mathbf{E}$  is a higher order polynomial with an order depending on the value N used for the exponential matrix in eq.(30) and on the number of mathematical layers M used in eqs.(31)-(32). The vector  $\mathbf{U}_1(0)$  contains the three displacement components and their derivatives with respect z calculated at the bottom ( $h^1=0$ ) of the first layer ( $j=1$ ):

$$\mathbf{U}_1(0) = [ U_1(0) \quad V_1(0) \quad W_1(0) \quad U'_1(0) \quad V'_1(0) \quad W'_1(0) ]^T, \quad (37)$$

The method is implemented in a Matlab code in the case of the spherical shell case, it automatically degenerates into cylindrical open/closed shell and plate methods.

The free vibration analysis is conducted finding the non-trivial solution of  $\mathbf{U}_1(0)$  in eq.(36), the determinant of matrix  $\mathbf{E}$  is imposed equal to zero:

$$\det[\mathbf{E}] = 0, \quad (38)$$

Eq.(38) allows to find the roots of an higher order polynomial in  $\lambda = \omega^2$ . For each pair of imposed half-wave numbers (m,n), a certain number of circular frequencies are obtained depending on the order N adopted for each exponential matrix  $\mathbf{A}^{j**}$ .

## 4 Results

Results given in this section allow to find the best values for the order of expansion N of the exponential matrix  $\mathbf{A}^{j**}$  described in eq.(30) and for the number of mathematical layers M used for the approximation of the shell curvature to obtain 3D equilibrium equations with constant coefficients. The M layers depend on the interlaminar continuity conditions as shown in eqs.(31) and (32).

The considered cases are simply supported square plates, cylindrical shell panels, cylinders and spherical shell panels. In-plane plate dimensions are  $a=b=1\text{m}$  with infinite radii of curvature  $R_\alpha$  and  $R_\beta$  and thickness ratios  $a/h=100$  and  $5$ . Cylindrical shell panels have radius of curvature in  $\alpha$ -direction  $R_\alpha=10\text{m}$  and an infinite radius of curvature  $R_\beta$  in  $\beta$ -direction. In plane dimensions are  $a=\pi/3R_\alpha$  and  $b=20\text{m}$ . Thickness ratios are  $R_\alpha/h=100$  and  $5$ . Cylinders have radius of curvature in  $\alpha$ -direction  $R_\alpha=10\text{m}$  and an infinite radius of curvature  $R_\beta$  in  $\beta$ -direction. In plane dimensions are  $a=2\pi R_\alpha$  and  $b=100\text{m}$ . Thickness ratios are  $R_\alpha/h=100$  and  $5$ . Spherical shell panels have radii of curvature  $R_\alpha=R_\beta=10\text{m}$ . In plane dimensions are  $a=b=\pi/3R_\alpha$ . Thickness ratios are  $R_\alpha/h=100$  and  $5$ . All these geometries have been considered as one-layered embedding an aluminium alloy with Young modulus  $E=73\text{GPa}$ , Poisson ratio  $\nu=0.3$  and mass density  $\rho=2800\text{kg/m}^3$ . Square plates and cylindrical shell panels have also been considered as sandwich configurations with external skins in aluminium alloy (same properties of the one-layered cases) and an internal soft core with Young modulus  $E=180\text{MPa}$ , Poisson ratio  $\nu=0.37$  and mass density  $\rho=50\text{kg/m}^3$ . The internal core has a thickness  $h_c=0.6h$  where  $h$  is the total thickness. Each external skin has thickness  $h_s=0.2h$ . Cylinders and spherical shell panels have also been considered as sandwich configurations with external composite skins and an internal soft core. The core has the same thickness and material properties already seen for the sandwich configuration with isotropic skins. The composite skins are made of two laminae at the bottom with fibre orientation  $0^\circ/90^\circ$  and thickness values  $h_{0^\circ}=h_{90^\circ}=0.1h$  and two laminae at the top with fibre orientation  $90^\circ/0^\circ$  and thickness values  $h_{90^\circ}=h_{0^\circ}=0.1h$ . The global lamination from the bottom to the top is  $0^\circ/90^\circ/\text{core}/90^\circ/0^\circ$ . The properties of the fibre reinforced composite material are Young moduli  $E_1=132.38\text{GPa}$  and  $E_2=E_3=10.756\text{GPa}$ , shear moduli  $G_{12}=G_{13}=5.6537\text{GPa}$  and  $G_{23}=3.603\text{GPa}$ , Poisson ratios  $\nu_{12}=\nu_{13}=0.24$  and  $\nu_{23}=0.43$  and mass density  $\rho=1600\text{kg/m}^3$ . All the sandwich configurations present the same thickness ratios already discussed for the one-layered isotropic

cases. Results in tables are given as dimensionless circular frequencies  $\bar{\omega} = \omega(a^2/h)\sqrt{\rho/E}$  for one-layered isotropic cases,  $\bar{\omega} = \omega(a^2/h)\sqrt{\rho_{skin}/E_{skin}}$  for the sandwich configurations with isotropic skins and  $\bar{\omega} = \omega(a^2/h)\sqrt{\rho_{skin}/E_{2skin}}$  for the sandwich configurations with composite skins.  $a$  is the in-plane dimension of the structure in the  $\alpha$  direction.  $h$  is the total thickness of the structure.  $\rho$  is the mass density of the aluminium alloy for the one-layered cases,  $\rho_{skin}$  is the mass density of the isotropic or composite skins.  $E$  is the Young modulus of the one-layered structure,  $E_{skin}$  is the Young modulus of the isotropic skin,  $E_{2skin}$  is the Young modulus in direction 2 for the composite skin. When the half-wave numbers  $m$  and  $n$  are imposed in the in-plane directions  $\alpha$  and  $\beta$ , circular frequencies  $\omega$  from I, II, III to  $\infty$  are obtained. In the visualization of vibration modes, the thickness coordinate is given in dimensionless form  $z^*=z/h$  and the three displacement components are also given in dimensionless form  $u^*=u/|U_{max}|$ ,  $v^*=v/|V_{max}|$  and  $w^*=w/|W_{max}|$ . In proposed tables, when the convergence is reached, the frequencies are indicated in bold. The use of NaN indicates "Not a Number" when there is a numerical problem for the solution developed with certain  $M$  and  $N$  values. In these cases the global matrix and the related system are not well conditioned.

One-layered structures have one physical layer ( $N_L=1$ ), this layer can be divided in several mathematical layers  $M$ . Figure 3 shows the use of 1 and 10 mathematical layers in the one-layered structures. Sandwich structures with isotropic skins have three physical layers ( $N_L=3$ ), these layers can be divided in  $M$  uniform mathematical layers. Figure 4 shows a shell structure with three physical layers divided in  $M=10$  mathematical layers. Sandwich structures with composite skins have five physical layers ( $N_L=5$ ), these layers can be divided in  $M$  uniform mathematical layers. Figure 5 shows a shell structure with five physical layers divided in  $M=10$  mathematical layers. For plate geometries the use of mathematical layers is not mandatory in order to apply the exponential matrix method for the solution of the system of partial differential equations. In fact, 3D equilibrium equations have constant coefficients. However, their use is also proposed in analogy to the shell cases in order to understand their possible advantages.

Table 1 shows the first frequency (I), for imposed half-wave numbers  $m=n=1$  and  $m=n=2$  and thickness ratios  $a/h$  equal 100 and 5, in the case of one-layered isotropic plate. In this case, the use of mathematical layers  $M$  is not necessary. For  $M=1$  (no mathematical layers), the convergence of the solution is obtained for an order of expansion for the exponential matrix  $N=5$  for thin plates ( $a/h=100$ ) and both combinations of half-wave numbers. Higher  $N$  values are necessary for thicker plates ( $a/h=5$ ), in particular  $N=9$  for  $m=n=1$  and  $N=11$  for  $m=n=2$ . The mathematical layers have also been considered, even if they are not necessary, to demonstrate that the use of mathematical layers allows to reduce the order  $N$  for the exponential matrix. For plate cases, it is more convenient, for computational reasons, the use of a higher  $N$  value and not the inclusion of  $M$  mathematical layers.

The first frequency (I) for imposed half-wave numbers  $m=n=1$  and  $m=n=2$  is proposed in Table 2 for the case of thin ( $R_\alpha/h=100$ ) and thick ( $R_\alpha/h=5$ ) isotropic one-layered cylindrical shell panels. For these geometries the use of  $M$  mathematical layers is mandatory to solve the system of partial differential equations with variable coefficients. The structure is one-layered and isotropic without transverse anisotropy. For these reasons,  $M=10$  mathematical layers are sufficient to approximate the curvature terms in the case of thin shell ( $R_\alpha/h=100$ ) and  $m=n=1$ .  $M=20$  mathematical layers are mandatory in the case of thin shell with  $m=n=2$ .  $N=3$  order of expansion is sufficient to correctly approximate the exponential matrix when  $M$  mathematical layers are employed. For thick shells ( $R_\alpha/h=5$ ), a higher  $M$  value for mathematical layers is necessary to approximate the curvature ( $M=60$  for  $m=n=1$  and  $M=20$  for  $m=n=2$ ).  $m$  and  $n$  effects demonstrate the dependence of the convergence from the type of vibration mode. This dependence is not a priori predictable. The first (I) vibration mode is shown in Figure 6 for the thick shell ( $R_\alpha/h=5$ ) and half-wave numbers  $m=n=1$  and  $m=n=2$ .

Table 3 shows the first frequency (I), for imposed half-wave numbers ( $m=2, n=1$ ) and ( $m=2, n=3$ ) and thickness ratios  $R_\alpha/h$  equal 100 and 5, in the case of one-layered isotropic cylinder. The number  $M$  of mathematical layers to approximate the curvature in cylinders is smaller than the cylindrical and spherical shell cases because of the symmetry of the cylinder geometry and its bigger rigidity. For thin

cylinders and  $m=2$  and  $n=1$ ,  $M=10$  mathematical layers are sufficient. For thin cylinder and  $m=2$  and  $n=3$ , mathematical layers are not necessary. In the case of thick cylinders, the  $M$  mathematical layers for a correct convergence increases until  $M=40$  for  $m=2$  and  $n=1$ . The case  $m=2$  and  $n=3$  shows the dependency of the convergence analysis from the half-wave numbers. For thick shells,  $N=3$  order for the exponential matrix combined with an opportune choice of the mathematical layers guarantee the desired convergence. Figure 7 shows the first (I) vibration mode for the thick shell ( $R_\alpha/h=5$ ) and couples of half-wave numbers ( $m=2$  and  $n=1$ ) and ( $m=2$  and  $n=3$ ).

The isotropic one-layered spherical shell is analyzed in Table 4. The first (I) frequency is investigated for imposed half-wave numbers  $m=n=1$  and  $m=n=2$  and thickness ratios  $R_\alpha/h$  equal 100 and 5. Conclusions similar to the cylindrical shell panels can be reached. For thin shells,  $M=10$  mathematical layers are sufficient for the curvature approximation.  $M=40$  mathematical layers must be used for thick shells in the case of  $m=n=1$ . For all these cases,  $N=3$  order of expansion for the exponential matrix method is sufficient for a correct analysis. When the number of mathematical layers  $M$  are not sufficient for a correct curvature approximation, even if  $N=12$  order of expansion is used, the correct solution is not obtained. Figure 8 shows the first frequency (I) for the thick isotropic spherical shell ( $R_\alpha/h=5$ ) and couples of half-wave numbers  $m=n=1$  and  $m=n=2$ .

Tables 1-4 have shown the effects of thickness ratio, half-wave numbers and geometry in the convergence analysis of the order of expansion  $N$  for the exponential matrix and the number of mathematical layers  $M$  for the curvature approximation. Tables 5-8 have been added to investigate the effect of the lamination sequence (number of layers, materials, transverse and in-plane anisotropy). For this aim, a sandwich configuration with isotropic skins for plates and cylindrical shell panels and a sandwich configuration with composite skins for cylinders and spherical shell panels have been investigated. In general, for the same geometry, thickness ratio and half-wave numbers, sandwich configurations need a great number of mathematical layers  $M$  and a higher order of expansion  $N$  for the exponential matrix with respect the same one-layered cases. These considerations come from the comparisons between Table 1 and Table 5, Table 2 and Table 6, Table 3 and Table 7, Table 4 and Table 8. Thick sandwich cylindrical shell ( $R_\alpha/h=5$ ) in Table 6 and thick sandwich spherical shell ( $R_\alpha/h=5$  and  $m=n=1$ ) in Table 8 need  $M=100$  mathematical layers for a correct result. Figure 9 shows the first frequency (I) for the thick sandwich spherical shell with composite skins for half-wave numbers  $m=n=1$  and  $m=n=2$ . For sandwich configurations, the zigzag form of displacements components through the thickness confirms the high transverse anisotropy of this lamination sequence.

Tables 9-12 allow the study of the frequency order effect on the choice of the number  $M$  of mathematical layers and the order  $N$  for the exponential matrix. Table 9 investigates the first four modes for  $m=n=1$  of the thick ( $a/h=5$ ) sandwich plate with isotropic skins. Table 10 shows the first four modes for  $m=n=1$  of the thick ( $R_\alpha/h=5$ ) sandwich cylindrical shell with isotropic skins. Table 11 analyzes the first four modes for  $m=2$  and  $n=1$  of the thick ( $R_\alpha/h=5$ ) sandwich cylinder with composite skins. Table 12 shows the first four modes for  $m=n=1$  of the thick ( $R_\alpha/h=5$ ) sandwich spherical shell with composite skins. From Tables 9-12, it is clear how the choice of  $M$  and  $N$  parameters could also depend on the considered mode and frequency order. The first four frequencies (for the same half-wave numbers  $m$  and  $n$ ) could have a different through-the-thickness behaviour of the displacement components, as indicated in Figures 10 and 11 for sandwich cylindrical shell with isotropic skins and sandwich spherical shell with composite skins, respectively. In the vibration mode visualization, the zigzag effect for sandwich structures (due to the transverse anisotropy) is clearly indicated. Convergence analysis has a strong dependency from the frequency order but this dependency is not a priori predictable because it depends on the vibration mode type.

The choice of  $M$  and  $N$  values depends on several parameters such as geometry, thickness ratio, lamination sequence, material, half-wave numbers, vibration mode and order of frequency.  $M$  and  $N$  values have a dependence from vibration mode and order of frequency that is not a priori predictable, in particular for very higher order modes (over the fourth one). For these reasons, a conservative choice

with  $M=100$  mathematical layers and  $N=3$  order of expansion for the exponential matrix, in order to analyze each configuration with an optimum for the residual errors and computational costs, has been made.  $M=100$  and  $N=3$  allow an exact analysis for each structure, thickness ratio, lamination sequence, material, half-wave numbers, mode and order of frequency, considering a low computational cost and time consumption. In the case of  $M=1$  mathematical layer, the method has a very low computation time which means that the results are obtained in few seconds for any  $N$  value for the expansion of the exponential matrix. The addition of  $M$  mathematical layers is more heavy from the computational point of view, e.g., a model with  $M=100$  and  $N=3$  has a computation time of about 60 seconds. These features are confirmed by the results in Tables 13-15 where the present 3D exact solution is compared with other 3D solutions given in the literature. Table 13 compares the present 3D exact solution with that by Messina [18] for a simply supported multilayered composite square plate ( $a/h=10$ ). The first three modes (I, II and III) for several lamination sequences and imposed half-wave numbers  $m$  and  $n$  are investigated. The present 3D results and Messina [18] results are always coincident. In this plate case, the use of mathematical layers is not necessary and  $M=2, 3$  and  $4$  are used (coincident with the number of physical layers  $N_L$ ). A  $N=12$  order for the exponential matrix has been used because the mathematical layers have not been introduced. This assessment considers a simply supported square plate ( $a=b=10$ ) with thickness ratio  $a/h=10$ . The plate is multilayered and each composite layer has Young modulus components  $E_1=25.1 \times 10^6$  psi,  $E_2=4.8 \times 10^6$  psi and  $E_3=0.75 \times 10^6$  psi, shear modulus components  $G_{12}=1.36 \times 10^6$  psi,  $G_{13}=1.2 \times 10^6$  psi and  $G_{23}=0.47 \times 10^6$  psi, Poisson ratio components  $\nu_{12} = 0.036$ ,  $\nu_{13} = 0.25$  and  $\nu_{23} = 0.171$ . The mass density is  $\rho=0.0541911$  lb/in<sup>3</sup>. The first three vibration modes are given in terms of dimensionless circular frequency  $\bar{\omega} = \omega h \sqrt{\rho/E_2}$  for half-wave numbers  $(m,n)$  equal  $(1,1)$ ,  $(1,2)$ ,  $(2,1)$  and  $(2,2)$ . Two-layered, three-layered and four-layered composite plates are investigated with lamination sequence  $(0^\circ/90^\circ)$ ,  $(0^\circ/90^\circ/0^\circ)$  and  $(0^\circ/90^\circ/0^\circ/90^\circ)$ , respectively (each layer has the same thickness). Tables 14 and 15 show the assessment proposed by Huang [23] for simply supported cylindrical and spherical shell panels, respectively. Cylindrical shell panel has radius of curvature  $R_\alpha=10$  and thickness  $h=0.5$ . The radius of curvature in  $\beta$  direction is infinite and the shell has dimensions  $a=b=5$ . The structure is multilayered (it embeds  $N_L$  layers) and each layer has the same thickness. The lamination sequence is  $(0^\circ/90^\circ/0^\circ/90^\circ/\dots)$ . Each composite layer has Young modulus components  $E_1=25E_0$  and  $E_2=E_3=E_0$ , shear modulus components  $G_{12}=G_{13}=0.5E_0$  and  $G_{23}=0.2E_0$ , Poisson ratio components  $\nu_{12} = \nu_{13} = \nu_{23} = 0.25$ . The mass density is  $\rho=1500$  kg/m<sup>3</sup>. The number of layers  $N_L$  is 2, 4 and 10. Spherical shell panel has radii of curvature  $R_\alpha=R_\beta=10$ , thickness  $h=0.2$  and dimensions  $a=b=2$ . The structure is multilayered (it embeds  $N_L$  layers) and each layer has the same thickness. The lamination sequence is  $(0^\circ/90^\circ/0^\circ/90^\circ/\dots)$ . The same material of the cylindrical shell is considered. In Tables 14 and 15, the present 3D solution and the 3D solution by Huang [23] are coincident for each geometry, thickness ratio, lamination sequence, half-wave numbers and frequency order.  $M=100$  mathematical layers and order  $N=3$  for the exponential matrix have been used.

## 5 Conclusions

The paper proposes the three-dimensional equilibrium equations written in general orthogonal curvilinear coordinates for the free vibration analysis of multilayered plates, cylinders and spherical/cylindrical shell panels. The system of differential equations has been solved by means of the exponential matrix method. The solution has been given in closed form considering simply supported structure and harmonic form for displacement components. The equilibrium equations have constant coefficients in the case of plate geometries and coefficients depending on the thickness coordinate  $z$  in the case of shell geometries. In the plate cases an opportune choice of the order of expansion  $N$  for the exponential matrix is mandatory. For shell cases, in addition to the order  $N$ , the opportune value  $M$  of mathematical layers must be identified to correctly solve the three-dimensional equations with variable coefficients. The opportune  $N$  and  $M$  values depend on several parameters such as geometry, thickness ratio, material,

lamination sequence, imposed half-wave numbers, frequency order and vibration mode. For plate cases, mathematical layers are not mandatory and  $N=12$  for the exponential matrix always allows the correct solution. In shell cases, the use of mathematical layers is mandatory in order to describe the curvature approximation. The use of  $M$  mathematical layers allows also the reduction of the order  $N$  for the exponential matrix.  $N=3$  gives always the correct solution if combined with an opportune value  $M$  for mathematical layers. However, the dependency of the mathematical layers from geometry, thickness ratio, material, lamination sequence, half-wave numbers, vibration mode and frequency order is not always a priori predictable. Therefore, the choice of  $M=100$  is set to have a conservative approach.

## Conflict of Interest

The author declares that he has no conflict of interest.

## References

- [1] F. Tornabene and N. Fantuzzi, *Mechanics of Laminated Composite Doubly-Curved Shell Structures. The Generalized Differential Quadrature Method and the Strong Formulation Finite Element Method*, Società Editrice Esculapio, Bologna (Italy), 2014.
- [2] F. Tornabene, *Meccanica delle Strutture a Guscio in Materiale Composito*, Società Editrice Esculapio, Bologna (Italy), 2012.
- [3] J.N. Reddy, *Mechanics of Laminated Composite Plates and Shells: Theory and Analysis*, CRC Press, 2nd Edition, New York, 2004.
- [4] E. Carrera, S. Brischetto and P. Nali, *Plates and Shells for Smart Structures: Classical and Advanced Theories for Modeling and Analysis*, John Wiley & Sons, Ltd., New Delhi, 2011.
- [5] G.B. Gustafson, *Systems of Differential Equations*, free available on <http://www.math.utah.edu/gustafso/2250systems-de.pdf>, accessed on 7th March 2016.
- [6] W.E. Boyce and R.C. DiPrima, *Elementary Differential Equations and Boundary Value Problems*, John Wiley & Sons, Ltd., New York, 2001.
- [7] D. Zwillinger, *Handbook of Differential Equations*, Academic Press, New York, 1997.
- [8] C. Molery and C. Van Loan, Nineteen dubious ways to compute the exponential of a matrix, twenty-five years later, *SIAM Review*, 45, 1-46, 2003.
- [9] S. Brischetto, Exact elasticity solution for natural frequencies of functionally graded simply-supported structures, *CMES: Computer Modeling in Engineering & Sciences*, 95, 391-430, 2013.
- [10] S. Brischetto, Three-dimensional exact free vibration analysis of spherical, cylindrical, and flat one-layered panels, *Shock and Vibration*, Vol. 2014, Article ID 479738, 1-29, 2014.
- [11] S. Brischetto, An exact 3D solution for free vibrations of multilayered cross-ply composite and sandwich plates and shells, *International Journal of Applied Mechanics*, 6, 1-42, 2014.
- [12] S. Brischetto, A continuum elastic three-dimensional model for natural frequencies of single-walled carbon nanotubes, *Composites Part B: Engineering*, 61, 222-228, 2014.
- [13] S. Brischetto, A continuum shell model including van der Waals interaction for free vibrations of double-walled carbon nanotubes, *CMES: Computer Modeling in Engineering & Sciences*, 104, 305-327, 2015.

- [14] S. Brischetto and R. Torre, Exact 3D solutions and finite element 2D models for free vibration analysis of plates and cylinders, *Curved and Layered Structures*, 1, 59-92, 2014.
- [15] F. Tornabene, S. Brischetto, N. Fantuzzi and E. Viola, Numerical and exact models for free vibration analysis of cylindrical and spherical shell panels, *Composites part B: Engineering*, 81, 231-250, 2015.
- [16] S. Brischetto, F. Tornabene, N. Fantuzzi and E. Viola, 3D exact and 2D generalized differential quadrature models for free vibration analysis of functionally graded plates and cylinders, *Meccanica*, on-line, 1-40, 2016.
- [17] S. Brischetto, F. Tornabene, N. Fantuzzi and M. Baccocchi, Refined 2D and exact 3D shell models for the free vibration analysis of single- and double-walled carbon nanotubes, *Technologies*, 3, 259-284, 2015.
- [18] A. Messina, Three dimensional free vibration analysis of cross-ply laminated plates through 2D and exact models, *3rd International Conference on Integrity, Reliability and Failure*, Porto (Portugal), 20-24 July 2009.
- [19] K.P. Soldatos and J. Ye, Axisymmetric static and dynamic analysis of laminated hollow cylinders composed of monoclinic elastic layers, *Journal of Sound and Vibration*, 184, 245-259, 1995.
- [20] W.-Q. Chen, H.-J. Ding and R.-Q. Xu, On exact analysis of free vibrations of embedded transversely isotropic cylindrical shells, *International Journal of Pressure Vessels and Piping*, 75, 961-966, 1998.
- [21] J.-R. Fan and J.-Y. Zhang, Exact solutions for thick laminated shells, *Science in China*, 35, 1343-1355, 1992.
- [22] B. Gasemzadeh, R. Azarafza, Y. Sahebi and A. Motallebi, Analysis of free vibration of cylindrical shells on the basis of three dimensional exact elasticity theory, *Indian Journal of Science and Technology*, 5, 3260-3262, 2012.
- [23] N.N. Huang, Exact analysis for three-dimensional free vibrations of cross-ply cylindrical and doubly-curved laminates, *Acta Mechanica*, 108, 23-34, 1995.
- [24] J.N. Sharma, D.K. Sharma and S.S. Dhaliwal, Three-dimensional free vibration analysis of a viscothermoelastic hollow sphere, *Open Journal of Acoustics*, 2, 12-24, 2012.
- [25] J.N. Sharma and N. Sharma, Three-dimensional free vibration analysis of a homogeneous transversally isotropic thermoelastic sphere, *Journal of Applied Mechanics*, 77, 1-9, 2010.
- [26] A.E. Armenakas, D.C. Gazis and G. Herrmann, *Free Vibrations of Circular Cylindrical Shells*, Pergamon Press, Oxford, 1969.
- [27] A. Bhimaraddi, A higher order theory for free vibration analysis of circular cylindrical shells, *International Journal of Solids and Structures*, 20, 623-630, 1984.
- [28] H. Zhou, W. Li, B. Lv and W.L. Li, Free vibrations of cylindrical shells with elastic-support boundary conditions, *Applied Acoustics*, 73, 751-756, 2012.
- [29] S.S. Vel, Exact elasticity solution for the vibration of functionally graded anisotropic cylindrical shells, *Composite Structures*, 92, 2712-2727, 2010.

- [30] C.T. Loy and K.Y. Lam, Vibration of thick cylindrical shells on the basis of three-dimensional theory of elasticity, *Journal of Sound and Vibration*, 226, 719-737, 1999.
- [31] Y. Wang, R. Xu, H. Ding and J. Chen, Three-dimensional exact solutions for free vibrations of simply supported magneto-electro-elastic cylindrical panels, *International Journal of Engineering Science*, 48, 1778-1796, 2010.
- [32] E. Efraim and M. Eisenberger, Exact vibration frequencies of segmented axisymmetric shells, *Thin-Walled Structures*, 44, 281-289, 2006.
- [33] J.-H. Kanga and A.W. Leissa, Three-dimensional vibrations of thick spherical shell segments with variable thickness, *International Journal of Solids and Structures*, 37, 4811-4823, 2000.
- [34] K.M. Liew, L.X. Peng and T.Y. Ng, Three-dimensional vibration analysis of spherical shell panels subjected to different boundary conditions, *International Journal of Mechanical Sciences*, 44, 2103-2117, 2002.
- [35] S. Aimmanee and R.C. Batra, Analytical solution for vibration of an incompressible isotropic linear elastic rectangular plate, and frequencies missed in previous solutions, *Journal of Sound and Vibration*, 302, 613-620, 2007.
- [36] R.C. Batra and S. Aimmanee, Letter to the Editor: Missing frequencies in previous exact solutions of free vibrations of simply supported rectangular plates, *Journal of Sound and Vibration*, 265, 887-896, 2003.
- [37] S. Srinivas, C.V. Joga Rao and A.K. Rao, An exact analysis for vibration of simply-supported homogeneous and laminated thick rectangular plates, *Journal of Sound and Vibration*, 12, 187-199, 1970.
- [38] S. Srinivas, A.K. Rao and C.V.J. Rao, Flexure of simply supported thick homogeneous and laminated rectangular plates, *Zeitschrift für Angewandte Mathematik und Mechanik*, 49, 449-458, 1969.
- [39] R.C. Batra, S. Vidoli and F. Vestroni, Plane wave solutions and modal analysis in higher order shear and normal deformable plate theories, *Journal of Sound and Vibration*, 257, 63-88, 2002.
- [40] J.Q. Ye, A three-dimensional free vibration analysis of cross-ply laminated rectangular plates with clamped edges, *Computer Methods in Applied Mechanics and Engineering*, 140, 383-392, 1997.
- [41] Y.K. Cheung and D. Zhou, Three-dimensional vibration analysis of cantilevered and completely free isosceles triangular plates, *International Journal of Solids and Structures*, 39, 673-687, 2002.
- [42] K.M. Liew and B. Yang, Three-dimensional elasticity solutions for free vibrations of circular plates: a polynomials-Ritz analysis, *Computer Methods in Applied Mechanics and Engineering*, 175, 189-201, 1999.
- [43] Y.B. Zhao, G.W. Wei and Y. Xiang, Discrete singular convolution for the prediction of high frequency vibration of plates, *International Journal of Solids and Structures*, 39, 65-88, 2002.
- [44] G.W. Wei, Y.B. Zhao and Y. Xiang, A novel approach for the analysis of high-frequency vibrations, *Journal of Sound and Vibration*, 257, 207-246, 2002.
- [45] H. Rokni Damavandi Taher, M. Omid, A.A. Zadpoor and A.A. Nikooyan, Short Communication: Free vibration of circular and annular plates with variable thickness and different combinations of boundary conditions, *Journal of Sound and Vibration*, 296, 1084-1092, 2006.

- [46] Y. Xing and B. Liu, New exact solutions for free vibrations of rectangular thin plates by symplectic dual method, *Acta Mechanica Sinica*, 25, 265-270, 2009.
- [47] Sh. Hosseini-Hashemi, H. Salehipour and S.R. Atashipour, Exact three-dimensional free vibration analysis of thick homogeneous plates coated by a functionally graded layer, *Acta Mechanica*, 223, 2153-2166, 2012.
- [48] S.S. Vel and R.C. Batra, Three-dimensional exact solution for the vibration of functionally graded rectangular plates, *Journal of Sound and Vibration*, 272, 703-730, 2004.
- [49] Y. Xu and D. Zhou, Three-dimensional elasticity solution of functionally graded rectangular plates with variable thickness, *Composite Structures*, 91, 56-65, 2009.
- [50] D. Haojiang, X. Rongqiao and C. Weiqiu, Exact solutions for free vibration of transversely isotropic piezoelectric circular plates, *Acta Mechanica Sinica*, 16, 142-147, 2000.
- [51] B.P. Baillargeon and S.S. Vel, Exact solution for the vibration and active damping of composite plates with piezoelectric shear actuators, *Journal of Sound and Vibration*, 282, 781-804, 2005.
- [52] W.Q. Chen, J.B. Cai, G.R. Ye and Y.F. Wang, Exact three-dimensional solutions of laminated orthotropic piezoelectric rectangular plates featuring interlaminar bonding imperfections modeled by a general spring layer, *International Journal of Solids and Structures*, 41, 5247-5263, 2004.
- [53] Z.-Q. Cheng, C.W. Lim and S. Kitipornchai, Three-dimensional exact solution for inhomogeneous and laminated piezoelectric plates, *International Journal of Engineering Science*, 37, 1425-1439, 1999.
- [54] S. Kapuria and P.G. Nair, Exact three-dimensional piezothermoelasticity solution for dynamics of rectangular cross-ply hybrid plates featuring interlaminar bonding imperfections, *Composites Science and Technology*, 70, 752-762, 2010.
- [55] Z. Zhong and E.T. Shang, Three-dimensional exact analysis of a simply supported functionally gradient piezoelectric plate, *International Journal of Solids and Structures*, 40, 5335-5352, 2003.
- [56] F.B. Hildebrand, E. Reissner and G.B. Thomas, *Notes on the Foundations of the Theory of Small Displacements of Orthotropic Shells*, NACA Technical Note No. 1833, Washington, 1949.
- [57] W. Soedel, *Vibration of Shells and Plates*, Marcel Dekker, Inc., New York, 2004.



m=1, n=1; a/h=100												
	N=1	N=2	N=3	N=4	N=5	N=6	N=7	N=8	N=9	N=10	N=11	N=12
M=1	275.54	10.341	5.9665	5.9724	<b>5.9713</b>	<b>5.9713</b>	<b>5.9713</b>	<b>5.9713</b>	<b>5.9713</b>	<b>5.9713</b>	<b>5.9713</b>	<b>5.9713</b>
M=10	5.9414	6.0306	<b>5.9713</b>	<b>5.9713</b>	<b>5.9713</b>	<b>5.9713</b>	<b>5.9713</b>	<b>5.9713</b>	<b>5.9713</b>	<b>5.9713</b>	<b>5.9713</b>	<b>5.9713</b>
M=20	5.9638	5.9862	<b>5.9713</b>	<b>5.9713</b>	<b>5.9713</b>	<b>5.9713</b>	<b>5.9713</b>	<b>5.9713</b>	<b>5.9713</b>	<b>5.9713</b>	<b>5.9713</b>	<b>5.9713</b>
M=40	5.9694	5.9750	<b>5.9713</b>	<b>5.9713</b>	<b>5.9713</b>	<b>5.9713</b>	<b>5.9713</b>	<b>5.9713</b>	<b>5.9713</b>	<b>5.9713</b>	<b>5.9713</b>	<b>5.9713</b>
M=60	5.9704	5.9729	<b>5.9713</b>	<b>5.9713</b>	<b>5.9713</b>	<b>5.9713</b>	<b>5.9713</b>	<b>5.9713</b>	<b>5.9713</b>	<b>5.9713</b>	<b>5.9713</b>	<b>5.9713</b>
M=80	5.9708	5.9722	<b>5.9713</b>	<b>5.9713</b>	<b>5.9713</b>	<b>5.9713</b>	<b>5.9713</b>	<b>5.9713</b>	<b>5.9713</b>	<b>5.9713</b>	<b>5.9713</b>	<b>5.9713</b>
M=100	5.9710	5.9719	<b>5.9713</b>	<b>5.9713</b>	<b>5.9713</b>	<b>5.9713</b>	<b>5.9713</b>	<b>5.9713</b>	<b>5.9713</b>	<b>5.9713</b>	<b>5.9713</b>	<b>5.9713</b>
m=1, n=1; a/h=5												
	N=1	N=2	N=3	N=4	N=5	N=6	N=7	N=8	N=9	N=10	N=11	N=12
M=1	13.777	8.8703	3.6564	5.6957	5.2506	5.3144	5.3027	5.3038	<b>5.3036</b>	<b>5.3036</b>	<b>5.3036</b>	<b>5.3036</b>
M=10	5.2915	5.3428	5.3035	<b>5.3036</b>	<b>5.3036</b>	<b>5.3036</b>	<b>5.3036</b>	<b>5.3036</b>	<b>5.3036</b>	<b>5.3036</b>	<b>5.3036</b>	<b>5.3036</b>
M=20	5.3006	5.3134	<b>5.3036</b>	<b>5.3036</b>	<b>5.3036</b>	<b>5.3036</b>	<b>5.3036</b>	<b>5.3036</b>	<b>5.3036</b>	<b>5.3036</b>	<b>5.3036</b>	<b>5.3036</b>
M=40	5.3029	5.3061	<b>5.3036</b>	<b>5.3036</b>	<b>5.3036</b>	<b>5.3036</b>	<b>5.3036</b>	<b>5.3036</b>	<b>5.3036</b>	<b>5.3036</b>	<b>5.3036</b>	<b>5.3036</b>
M=60	5.3033	5.3047	<b>5.3036</b>	<b>5.3036</b>	<b>5.3036</b>	<b>5.3036</b>	<b>5.3036</b>	<b>5.3036</b>	<b>5.3036</b>	<b>5.3036</b>	<b>5.3036</b>	<b>5.3036</b>
M=80	5.3034	5.3042	<b>5.3036</b>	<b>5.3036</b>	<b>5.3036</b>	<b>5.3036</b>	<b>5.3036</b>	<b>5.3036</b>	<b>5.3036</b>	<b>5.3036</b>	<b>5.3036</b>	<b>5.3036</b>
M=100	5.3035	5.3040	<b>5.3036</b>	<b>5.3036</b>	<b>5.3036</b>	<b>5.3036</b>	<b>5.3036</b>	<b>5.3036</b>	<b>5.3036</b>	<b>5.3036</b>	<b>5.3036</b>	<b>5.3036</b>
m=2, n=2; a/h=100												
	N=1	N=2	N=3	N=4	N=5	N=6	N=7	N=8	N=9	N=10	N=11	N=12
M=1	551.07	41.309	23.785	23.879	<b>23.860</b>	<b>23.860</b>	<b>23.860</b>	<b>23.860</b>	<b>23.860</b>	<b>23.860</b>	<b>23.860</b>	<b>23.860</b>
M=10	23.741	24.097	<b>23.860</b>	<b>23.860</b>	<b>23.860</b>	<b>23.860</b>	<b>23.860</b>	<b>23.860</b>	<b>23.860</b>	<b>23.860</b>	<b>23.860</b>	<b>23.860</b>
M=20	23.830	23.919	<b>23.860</b>	<b>23.860</b>	<b>23.860</b>	<b>23.860</b>	<b>23.860</b>	<b>23.860</b>	<b>23.860</b>	<b>23.860</b>	<b>23.860</b>	<b>23.860</b>
M=40	23.853	23.875	<b>23.860</b>	<b>23.860</b>	<b>23.860</b>	<b>23.860</b>	<b>23.860</b>	<b>23.860</b>	<b>23.860</b>	<b>23.860</b>	<b>23.860</b>	<b>23.860</b>
M=60	23.857	23.867	<b>23.860</b>	<b>23.860</b>	<b>23.860</b>	<b>23.860</b>	<b>23.860</b>	<b>23.860</b>	<b>23.860</b>	<b>23.860</b>	<b>23.860</b>	<b>23.860</b>
M=80	23.858	23.864	<b>23.860</b>	<b>23.860</b>	<b>23.860</b>	<b>23.860</b>	<b>23.860</b>	<b>23.860</b>	<b>23.860</b>	<b>23.860</b>	<b>23.860</b>	<b>23.860</b>
M=100	23.859	23.862	<b>23.860</b>	<b>23.860</b>	<b>23.860</b>	<b>23.860</b>	<b>23.860</b>	<b>23.860</b>	<b>23.860</b>	<b>23.860</b>	<b>23.860</b>	<b>23.860</b>
m=2, n=2; a/h=5												
	N=1	N=2	N=3	N=4	N=5	N=6	N=7	N=8	N=9	N=10	N=11	N=12
M=1	27.554	26.741	27.554	20.502	14.792	17.339	16.777	16.904	16.878	16.883	<b>16.882</b>	<b>16.882</b>
M=10	16.902	16.951	16.881	<b>16.882</b>	<b>16.882</b>	<b>16.882</b>	<b>16.882</b>	<b>16.882</b>	<b>16.882</b>	<b>16.882</b>	<b>16.882</b>	<b>16.882</b>
M=20	16.887	16.899	<b>16.882</b>	<b>16.882</b>	<b>16.882</b>	<b>16.882</b>	<b>16.882</b>	<b>16.882</b>	<b>16.882</b>	<b>16.882</b>	<b>16.882</b>	<b>16.882</b>
M=40	16.883	16.886	<b>16.882</b>	<b>16.882</b>	<b>16.882</b>	<b>16.882</b>	<b>16.882</b>	<b>16.882</b>	<b>16.882</b>	<b>16.882</b>	<b>16.882</b>	<b>16.882</b>
M=60	16.882	16.884	<b>16.882</b>	<b>16.882</b>	<b>16.882</b>	<b>16.882</b>	<b>16.882</b>	<b>16.882</b>	<b>16.882</b>	<b>16.882</b>	<b>16.882</b>	<b>16.882</b>
M=80	16.882	16.883	<b>16.882</b>	<b>16.882</b>	<b>16.882</b>	<b>16.882</b>	<b>16.882</b>	<b>16.882</b>	<b>16.882</b>	<b>16.882</b>	<b>16.882</b>	<b>16.882</b>
M=100	16.882	16.883	<b>16.882</b>	<b>16.882</b>	<b>16.882</b>	<b>16.882</b>	<b>16.882</b>	<b>16.882</b>	<b>16.882</b>	<b>16.882</b>	<b>16.882</b>	<b>16.882</b>

Table 1: One-layered isotropic plate. First mode (I) given as dimensionless circular frequency  $\bar{\omega} = \omega(a^2/h)\sqrt{\rho/E}$ . One physical layer ( $N_L=1$ ) divided in M mathematical layers.

m=1, n=1; R <sub>α</sub> /h=100												
	N=1	N=2	N=3	N=4	N=5	N=6	N=7	N=8	N=9	N=10	N=11	N=12
M=1	10.250	23.069	22.531	22.536	22.535	22.535	22.535	22.535	22.535	22.535	22.535	22.535
M=10	21.618	22.509	<b>22.503</b>	<b>22.503</b>	<b>22.503</b>	<b>22.503</b>	<b>22.503</b>	<b>22.503</b>	<b>22.503</b>	<b>22.503</b>	<b>22.503</b>	<b>22.503</b>
M=20	22.065	22.505	<b>22.503</b>	<b>22.503</b>	<b>22.503</b>	<b>22.503</b>	<b>22.503</b>	<b>22.503</b>	<b>22.503</b>	<b>22.503</b>	<b>22.503</b>	<b>22.503</b>
M=40	22.286	22.504	<b>22.503</b>	<b>22.503</b>	<b>22.503</b>	<b>22.503</b>	<b>22.503</b>	<b>22.503</b>	<b>22.503</b>	<b>22.503</b>	<b>22.503</b>	<b>22.503</b>
M=60	22.358	<b>22.503</b>	<b>22.503</b>	<b>22.503</b>	<b>22.503</b>	<b>22.503</b>	<b>22.503</b>	<b>22.503</b>	<b>22.503</b>	<b>22.503</b>	<b>22.503</b>	<b>22.503</b>
M=80	22.395	<b>22.503</b>	<b>22.503</b>	<b>22.503</b>	<b>22.503</b>	<b>22.503</b>	<b>22.503</b>	<b>22.503</b>	<b>22.503</b>	<b>22.503</b>	<b>22.503</b>	<b>22.503</b>
M=100	22.416	<b>22.503</b>	<b>22.503</b>	<b>22.503</b>	<b>22.503</b>	<b>22.503</b>	<b>22.503</b>	<b>22.503</b>	<b>22.503</b>	<b>22.503</b>	<b>22.503</b>	<b>22.503</b>
m=1, n=1; R <sub>α</sub> /h=5												
	N=1	N=2	N=3	N=4	N=5	N=6	N=7	N=8	N=9	N=10	N=11	N=12
M=1	11.746	6.2291	1.6677	3.6225	3.3365	3.3787	3.3508	3.3576	98.316	0.0105	NaN	0.0000
M=10	0.0105	2.9510	339.58	3.2167	3.2173	3.2172	3.2172	3.2172	3.2172	3.2172	3.2172	3.2172
M=20	339.58	3.2231	3.2159	3.2160	3.2160	3.2160	3.2160	3.2160	3.2160	3.2160	3.2160	3.2160
M=40	3.1533	3.2174	3.2157	3.2157	3.2157	3.2157	3.2157	3.2157	3.2157	3.2157	3.2157	3.2157
M=60	3.1743	3.2164	<b>3.2156</b>	<b>3.2156</b>	<b>3.2156</b>	<b>3.2156</b>	<b>3.2156</b>	<b>3.2156</b>	<b>3.2156</b>	<b>3.2156</b>	<b>3.2156</b>	<b>3.2156</b>
M=80	3.1847	3.2160	<b>3.2156</b>	<b>3.2156</b>	<b>3.2156</b>	<b>3.2156</b>	<b>3.2156</b>	<b>3.2156</b>	<b>3.2156</b>	<b>3.2156</b>	<b>3.2156</b>	<b>3.2156</b>
M=100	3.1910	3.2159	<b>3.2156</b>	<b>3.2156</b>	<b>3.2156</b>	<b>3.2156</b>	<b>3.2156</b>	<b>3.2156</b>	<b>3.2156</b>	<b>3.2156</b>	<b>3.2156</b>	<b>3.2156</b>
m=2, n=2; R <sub>α</sub> /h=100												
	N=1	N=2	N=3	N=4	N=5	N=6	N=7	N=8	N=9	N=10	N=11	N=12
M=1	463.87	34.817	27.498	27.585	27.581	27.581	27.581	27.581	27.581	27.581	27.581	27.581
M=10	23.623	27.532	27.452	27.452	27.452	27.452	27.452	27.452	27.452	27.452	27.452	27.452
M=20	25.619	27.471	<b>27.451</b>	<b>27.451</b>	<b>27.451</b>	<b>27.451</b>	<b>27.451</b>	<b>27.451</b>	<b>27.451</b>	<b>27.451</b>	<b>27.451</b>	<b>27.451</b>
M=40	26.554	27.456	<b>27.451</b>	<b>27.451</b>	<b>27.451</b>	<b>27.451</b>	<b>27.451</b>	<b>27.451</b>	<b>27.451</b>	<b>27.451</b>	<b>27.451</b>	<b>27.451</b>
M=60	26.857	27.453	<b>27.451</b>	<b>27.451</b>	<b>27.451</b>	<b>27.451</b>	<b>27.451</b>	<b>27.451</b>	<b>27.451</b>	<b>27.451</b>	<b>27.451</b>	<b>27.451</b>
M=80	27.007	27.452	<b>27.451</b>	<b>27.451</b>	<b>27.451</b>	<b>27.451</b>	<b>27.451</b>	<b>27.451</b>	<b>27.451</b>	<b>27.451</b>	<b>27.451</b>	<b>27.451</b>
M=100	27.096	27.452	<b>27.451</b>	<b>27.451</b>	<b>27.451</b>	<b>27.451</b>	<b>27.451</b>	<b>27.451</b>	<b>27.451</b>	<b>27.451</b>	<b>27.451</b>	<b>27.451</b>
m=2, n=2; R <sub>α</sub> /h=5												
	N=1	N=2	N=3	N=4	N=5	N=6	N=7	N=8	N=9	N=10	N=11	N=12
M=1	23.140	20.061	23.187	14.158	10.797	11.906	11.694	11.742	114.69	0.0885	NaN	NaN
M=10	11.423	339.58	11.642	11.644	11.644	11.644	11.644	11.644	11.644	11.644	11.644	11.644
M=20	339.58	11.661	<b>11.643</b>	<b>11.643</b>	<b>11.643</b>	<b>11.643</b>	<b>11.643</b>	<b>11.643</b>	<b>11.643</b>	<b>11.643</b>	<b>11.643</b>	<b>11.643</b>
M=40	11.589	11.647	<b>11.643</b>	<b>11.643</b>	<b>11.643</b>	<b>11.643</b>	<b>11.643</b>	<b>11.643</b>	<b>11.643</b>	<b>11.643</b>	<b>11.643</b>	<b>11.643</b>
M=60	11.607	11.645	<b>11.643</b>	<b>11.643</b>	<b>11.643</b>	<b>11.643</b>	<b>11.643</b>	<b>11.643</b>	<b>11.643</b>	<b>11.643</b>	<b>11.643</b>	<b>11.643</b>
M=80	11.616	11.644	<b>11.643</b>	<b>11.643</b>	<b>11.643</b>	<b>11.643</b>	<b>11.643</b>	<b>11.643</b>	<b>11.643</b>	<b>11.643</b>	<b>11.643</b>	<b>11.643</b>
M=100	11.621	11.644	<b>11.643</b>	<b>11.643</b>	<b>11.643</b>	<b>11.643</b>	<b>11.643</b>	<b>11.643</b>	<b>11.643</b>	<b>11.643</b>	<b>11.643</b>	<b>11.643</b>

Table 2: One-layered isotropic cylindrical shell. First mode (I) given as dimensionless circular frequency  $\bar{\omega} = \omega(a^2/h)\sqrt{\rho/E}$ . One physical layer ( $N_L=1$ ) divided in M mathematical layers.

m=2, n=1; R <sub>α</sub> /h=100												
	N=1	N=2	N=3	N=4	N=5	N=6	N=7	N=8	N=9	N=10	N=11	N=12
M=1	246.46	244.62	244.60	244.60	244.60	244.60	244.60	244.60	244.60	244.60	244.60	244.60
M=10	244.78	<b>244.59</b>	<b>244.59</b>	<b>244.59</b>	<b>244.59</b>	<b>244.59</b>	<b>244.59</b>	<b>244.59</b>	<b>244.59</b>	<b>244.59</b>	<b>244.59</b>	<b>244.59</b>
M=20	244.69	<b>244.59</b>	<b>244.59</b>	<b>244.59</b>	<b>244.59</b>	<b>244.59</b>	<b>244.59</b>	<b>244.59</b>	<b>244.59</b>	<b>244.59</b>	<b>244.59</b>	<b>244.59</b>
M=40	244.64	<b>244.59</b>	<b>244.59</b>	<b>244.59</b>	<b>244.59</b>	<b>244.59</b>	<b>244.59</b>	<b>244.59</b>	<b>244.59</b>	<b>244.59</b>	<b>244.59</b>	<b>244.59</b>
M=60	244.63	<b>244.59</b>	<b>244.59</b>	<b>244.59</b>	<b>244.59</b>	<b>244.59</b>	<b>244.59</b>	<b>244.59</b>	<b>244.59</b>	<b>244.59</b>	<b>244.59</b>	<b>244.59</b>
M=80	244.62	<b>244.59</b>	<b>244.59</b>	<b>244.59</b>	<b>244.59</b>	<b>244.59</b>	<b>244.59</b>	<b>244.59</b>	<b>244.59</b>	<b>244.59</b>	<b>244.59</b>	<b>244.59</b>
M=100	244.61	<b>244.59</b>	<b>244.59</b>	<b>244.59</b>	<b>244.59</b>	<b>244.59</b>	<b>244.59</b>	<b>244.59</b>	<b>244.59</b>	<b>244.59</b>	<b>244.59</b>	<b>244.59</b>
m=2, n=1; R <sub>α</sub> /h=5												
	N=1	N=2	N=3	N=4	N=5	N=6	N=7	N=8	N=9	N=10	N=11	N=12
M=1	13.744	12.906	12.367	12.426	12.417	12.418	13.526	10.694	0.0061	5146.1	NaN	0.0000
M=10	12.322	12225	12.297	12.297	12.297	12.297	12.297	12.297	12.297	12.297	12.297	12.297
M=20	12225	12.297	12.296	12.296	12.296	12.296	12.296	12.296	12.296	12.296	12.296	12.296
M=40	12.342	12.296	<b>12.295</b>	<b>12.295</b>	<b>12.295</b>	<b>12.295</b>	<b>12.295</b>	<b>12.295</b>	<b>12.295</b>	<b>12.295</b>	<b>12.295</b>	<b>12.295</b>
M=60	12.327	<b>12.295</b>	<b>12.295</b>	<b>12.295</b>	<b>12.295</b>	<b>12.295</b>	<b>12.295</b>	<b>12.295</b>	<b>12.295</b>	<b>12.295</b>	<b>12.295</b>	<b>12.295</b>
M=80	12.319	<b>12.295</b>	<b>12.295</b>	<b>12.295</b>	<b>12.295</b>	<b>12.295</b>	<b>12.295</b>	<b>12.295</b>	<b>12.295</b>	<b>12.295</b>	<b>12.295</b>	<b>12.295</b>
M=100	12.314	<b>12.295</b>	<b>12.295</b>	<b>12.295</b>	<b>12.295</b>	<b>12.295</b>	<b>12.295</b>	<b>12.295</b>	<b>12.295</b>	<b>12.295</b>	<b>12.295</b>	<b>12.295</b>
m=2, n=3; R <sub>α</sub> /h=100												
	N=1	N=2	N=3	N=4	N=5	N=6	N=7	N=8	N=9	N=10	N=11	N=12
M=1	1355.3	<b>1353.7</b>	<b>1353.7</b>	<b>1353.7</b>	<b>1353.7</b>	<b>1353.7</b>	<b>1353.7</b>	<b>1353.7</b>	<b>1353.7</b>	<b>1353.7</b>	<b>1353.7</b>	<b>1353.7</b>
M=10	1353.8	<b>1353.7</b>	<b>1353.7</b>	<b>1353.7</b>	<b>1353.7</b>	<b>1353.7</b>	<b>1353.7</b>	<b>1353.7</b>	<b>1353.7</b>	<b>1353.7</b>	<b>1353.7</b>	<b>1353.7</b>
M=20	1353.8	<b>1353.7</b>	<b>1353.7</b>	<b>1353.7</b>	<b>1353.7</b>	<b>1353.7</b>	<b>1353.7</b>	<b>1353.7</b>	<b>1353.7</b>	<b>1353.7</b>	<b>1353.7</b>	<b>1353.7</b>
M=40	<b>1353.7</b>	<b>1353.7</b>	<b>1353.7</b>	<b>1353.7</b>	<b>1353.7</b>	<b>1353.7</b>	<b>1353.7</b>	<b>1353.7</b>	<b>1353.7</b>	<b>1353.7</b>	<b>1353.7</b>	<b>1353.7</b>
M=60	<b>1353.7</b>	<b>1353.7</b>	<b>1353.7</b>	<b>1353.7</b>	<b>1353.7</b>	<b>1353.7</b>	<b>1353.7</b>	<b>1353.7</b>	<b>1353.7</b>	<b>1353.7</b>	<b>1353.7</b>	<b>1353.7</b>
M=80	<b>1353.7</b>	<b>1353.7</b>	<b>1353.7</b>	<b>1353.7</b>	<b>1353.7</b>	<b>1353.7</b>	<b>1353.7</b>	<b>1353.7</b>	<b>1353.7</b>	<b>1353.7</b>	<b>1353.7</b>	<b>1353.7</b>
M=100	<b>1353.7</b>	<b>1353.7</b>	<b>1353.7</b>	<b>1353.7</b>	<b>1353.7</b>	<b>1353.7</b>	<b>1353.7</b>	<b>1353.7</b>	<b>1353.7</b>	<b>1353.7</b>	<b>1353.7</b>	<b>1353.7</b>
m=2, n=3; R <sub>α</sub> /h=5												
	N=1	N=2	N=3	N=4	N=5	N=6	N=7	N=8	N=9	N=10	N=11	N=12
M=1	69.179	70.225	68.025	68.353	68.313	68.317	74.740	62.888	0.0791	4928.9	NaN	NaN
M=10	68.686	12225	<b>68.323</b>	<b>68.323</b>	<b>68.323</b>	<b>68.323</b>	<b>68.323</b>	<b>68.323</b>	<b>68.323</b>	<b>68.323</b>	<b>68.323</b>	<b>68.323</b>
M=20	0.0000	68.326	<b>68.323</b>	<b>68.323</b>	<b>68.323</b>	<b>68.323</b>	<b>68.323</b>	<b>68.323</b>	<b>68.323</b>	<b>68.323</b>	<b>68.323</b>	<b>68.323</b>
M=40	68.366	68.324	<b>68.323</b>	<b>68.323</b>	<b>68.323</b>	<b>68.323</b>	<b>68.323</b>	<b>68.323</b>	<b>68.323</b>	<b>68.323</b>	<b>68.323</b>	<b>68.323</b>
M=60	68.352	<b>68.323</b>	<b>68.323</b>	<b>68.323</b>	<b>68.323</b>	<b>68.323</b>	<b>68.323</b>	<b>68.323</b>	<b>68.323</b>	<b>68.323</b>	<b>68.323</b>	<b>68.323</b>
M=80	68.345	<b>68.323</b>	<b>68.323</b>	<b>68.323</b>	<b>68.323</b>	<b>68.323</b>	<b>68.323</b>	<b>68.323</b>	<b>68.323</b>	<b>68.323</b>	<b>68.323</b>	<b>68.323</b>
M=100	68.340	<b>68.323</b>	<b>68.323</b>	<b>68.323</b>	<b>68.323</b>	<b>68.323</b>	<b>68.323</b>	<b>68.323</b>	<b>68.323</b>	<b>68.323</b>	<b>68.323</b>	<b>68.323</b>

Table 3: One-layered isotropic cylinder. First mode (I) given as dimensionless circular frequency  $\bar{\omega} = \omega(a^2/h)\sqrt{\rho/E}$ . One physical layer ( $N_L=1$ ) divided in M mathematical layers.

m=1, n=1; R <sub>α</sub> /h=100												
	N=1	N=2	N=3	N=4	N=5	N=6	N=7	N=8	N=9	N=10	N=11	N=12
M=1	100.93	105.07	104.76	104.77	104.77	104.77	104.77	104.77	104.77	104.77	104.77	104.77
M=10	104.39	<b>104.76</b>	<b>104.76</b>	<b>104.76</b>	<b>104.76</b>	<b>104.76</b>	<b>104.76</b>	<b>104.76</b>	<b>104.76</b>	<b>104.76</b>	<b>104.76</b>	<b>104.76</b>
M=20	104.57	<b>104.76</b>	<b>104.76</b>	<b>104.76</b>	<b>104.76</b>	<b>104.76</b>	<b>104.76</b>	<b>104.76</b>	<b>104.76</b>	<b>104.76</b>	<b>104.76</b>	<b>104.76</b>
M=40	104.67	<b>104.76</b>	<b>104.76</b>	<b>104.76</b>	<b>104.76</b>	<b>104.76</b>	<b>104.76</b>	<b>104.76</b>	<b>104.76</b>	<b>104.76</b>	<b>104.76</b>	<b>104.76</b>
M=60	104.70	<b>104.76</b>	<b>104.76</b>	<b>104.76</b>	<b>104.76</b>	<b>104.76</b>	<b>104.76</b>	<b>104.76</b>	<b>104.76</b>	<b>104.76</b>	<b>104.76</b>	<b>104.76</b>
M=80	104.71	<b>104.76</b>	<b>104.76</b>	<b>104.76</b>	<b>104.76</b>	<b>104.76</b>	<b>104.76</b>	<b>104.76</b>	<b>104.76</b>	<b>104.76</b>	<b>104.76</b>	<b>104.76</b>
M=100	104.72	<b>104.76</b>	<b>104.76</b>	<b>104.76</b>	<b>104.76</b>	<b>104.76</b>	<b>104.76</b>	<b>104.76</b>	<b>104.76</b>	<b>104.76</b>	<b>104.76</b>	<b>104.76</b>
m=1, n=1; R <sub>α</sub> /h=5												
	N=1	N=2	N=3	N=4	N=5	N=6	N=7	N=8	N=9	N=10	N=11	N=12
M=1	14.338	11.405	2.8057	7.6892	6.8984	7.0697	7.0570	7.0893	0.0799	0.0277	NaN	NaN
M=10	6.7664	339.58	6.9553	6.9564	6.9563	6.9563	6.9563	6.9563	6.9563	6.9563	6.9563	6.9563
M=20	0.0000	6.9629	6.9555	6.9556	6.9556	6.9556	6.9556	6.9556	6.9556	6.9556	6.9556	6.9556
M=40	6.9095	6.9572	<b>6.9554</b>	<b>6.9554</b>	<b>6.9554</b>	<b>6.9554</b>	<b>6.9554</b>	<b>6.9554</b>	<b>6.9554</b>	<b>6.9554</b>	<b>6.9554</b>	<b>6.9554</b>
M=60	6.92249	6.9562	<b>6.9554</b>	<b>6.9554</b>	<b>6.9554</b>	<b>6.9554</b>	<b>6.9554</b>	<b>6.9554</b>	<b>6.9554</b>	<b>6.9554</b>	<b>6.9554</b>	<b>6.9554</b>
M=80	6.9325	6.9558	<b>6.9554</b>	<b>6.9554</b>	<b>6.9554</b>	<b>6.9554</b>	<b>6.9554</b>	<b>6.9554</b>	<b>6.9554</b>	<b>6.9554</b>	<b>6.9554</b>	<b>6.9554</b>
M=100	6.9371	6.9556	<b>6.9554</b>	<b>6.9554</b>	<b>6.9554</b>	<b>6.9554</b>	<b>6.9554</b>	<b>6.9554</b>	<b>6.9554</b>	<b>6.9554</b>	<b>6.9554</b>	<b>6.9554</b>
m=2, n=2; R <sub>α</sub> /h=100												
	N=1	N=2	N=3	N=4	N=5	N=6	N=7	N=8	N=9	N=10	N=11	N=12
M=1	88.738	115.87	110.74	110.84	110.83	110.83	110.83	110.83	110.83	110.83	110.83	110.83
M=10	109.00	110.82	<b>110.77</b>	<b>110.77</b>	<b>110.77</b>	<b>110.77</b>	<b>110.77</b>	<b>110.77</b>	<b>110.77</b>	<b>110.77</b>	<b>110.77</b>	<b>110.77</b>
M=20	109.90	110.79	<b>110.77</b>	<b>110.77</b>	<b>110.77</b>	<b>110.77</b>	<b>110.77</b>	<b>110.77</b>	<b>110.77</b>	<b>110.77</b>	<b>110.77</b>	<b>110.77</b>
M=40	110.34	110.78	<b>110.77</b>	<b>110.77</b>	<b>110.77</b>	<b>110.77</b>	<b>110.77</b>	<b>110.77</b>	<b>110.77</b>	<b>110.77</b>	<b>110.77</b>	<b>110.77</b>
M=60	110.48	<b>110.77</b>	<b>110.77</b>	<b>110.77</b>	<b>110.77</b>	<b>110.77</b>	<b>110.77</b>	<b>110.77</b>	<b>110.77</b>	<b>110.77</b>	<b>110.77</b>	<b>110.77</b>
M=80	110.56	<b>110.77</b>	<b>110.77</b>	<b>110.77</b>	<b>110.77</b>	<b>110.77</b>	<b>110.77</b>	<b>110.77</b>	<b>110.77</b>	<b>110.77</b>	<b>110.77</b>	<b>110.77</b>
M=100	110.60	<b>110.77</b>	<b>110.77</b>	<b>110.77</b>	<b>110.77</b>	<b>110.77</b>	<b>110.77</b>	<b>110.77</b>	<b>110.77</b>	<b>110.77</b>	<b>110.77</b>	<b>110.77</b>
m=2, n=2; R <sub>α</sub> /h=5												
	N=1	N=2	N=3	N=4	N=5	N=6	N=7	N=8	N=9	N=10	N=11	N=12
M=1	28.809	28.870	28.856	23.041	11.982	18.387	17.341	17.621	112.78	122.00	NaN	NaN
M=10	17.370	0.0000	17.509	17.514	<b>17.513</b>	<b>17.513</b>	<b>17.513</b>	<b>17.513</b>	<b>17.513</b>	<b>17.513</b>	<b>17.513</b>	<b>17.513</b>
M=20	339.58	17.533	17.512	<b>17.513</b>	<b>17.513</b>	<b>17.513</b>	<b>17.513</b>	<b>17.513</b>	<b>17.513</b>	<b>17.513</b>	<b>17.513</b>	<b>17.513</b>
M=40	17.472	17.518	<b>17.513</b>	<b>17.513</b>	<b>17.513</b>	<b>17.513</b>	<b>17.513</b>	<b>17.513</b>	<b>17.513</b>	<b>17.513</b>	<b>17.513</b>	<b>17.513</b>
M=60	17.486	17.515	<b>17.513</b>	<b>17.513</b>	<b>17.513</b>	<b>17.513</b>	<b>17.513</b>	<b>17.513</b>	<b>17.513</b>	<b>17.513</b>	<b>17.513</b>	<b>17.513</b>
M=80	17.492	17.514	<b>17.513</b>	<b>17.513</b>	<b>17.513</b>	<b>17.513</b>	<b>17.513</b>	<b>17.513</b>	<b>17.513</b>	<b>17.513</b>	<b>17.513</b>	<b>17.513</b>
M=100	17.496	17.514	<b>17.513</b>	<b>17.513</b>	<b>17.513</b>	<b>17.513</b>	<b>17.513</b>	<b>17.513</b>	<b>17.513</b>	<b>17.513</b>	<b>17.513</b>	<b>17.513</b>

Table 4: One-layered isotropic spherical shell. First mode (I) given as dimensionless circular frequency  $\bar{\omega} = \omega(a^2/h)\sqrt{\rho/E}$ . One physical layer ( $N_L=1$ ) divided in M mathematical layers.

m=1, n=1; a/h=100												
	N=1	N=2	N=3	N=4	N=5	N=6	N=7	N=8	N=9	N=10	N=11	N=12
M=3	7.6313	7.9087	<b>7.7266</b>	<b>7.7266</b>	<b>7.7266</b>	<b>7.7266</b>	<b>7.7266</b>	<b>7.7266</b>	<b>7.7266</b>	<b>7.7266</b>	<b>7.7266</b>	<b>7.7266</b>
M=10	7.7040	7.7715	<b>7.7266</b>	<b>7.7266</b>	<b>7.7266</b>	<b>7.7266</b>	<b>7.7266</b>	<b>7.7266</b>	<b>7.7266</b>	<b>7.7266</b>	<b>7.7266</b>	<b>7.7266</b>
M=20	7.7209	7.7378	<b>7.7266</b>	<b>7.7266</b>	<b>7.7266</b>	<b>7.7266</b>	<b>7.7266</b>	<b>7.7266</b>	<b>7.7266</b>	<b>7.7266</b>	<b>7.7266</b>	<b>7.7266</b>
M=40	7.7252	7.7294	<b>7.7266</b>	<b>7.7266</b>	<b>7.7266</b>	<b>7.7266</b>	<b>7.7266</b>	<b>7.7266</b>	<b>7.7266</b>	<b>7.7266</b>	<b>7.7266</b>	<b>7.7266</b>
M=60	7.7259	7.7278	<b>7.7266</b>	<b>7.7266</b>	<b>7.7266</b>	<b>7.7266</b>	<b>7.7266</b>	<b>7.7266</b>	<b>7.7266</b>	<b>7.7266</b>	<b>7.7266</b>	<b>7.7266</b>
M=80	7.7262	7.7273	<b>7.7266</b>	<b>7.7266</b>	<b>7.7266</b>	<b>7.7266</b>	<b>7.7266</b>	<b>7.7266</b>	<b>7.7266</b>	<b>7.7266</b>	<b>7.7266</b>	<b>7.7266</b>
M=100	7.7263	7.7270	<b>7.7266</b>	<b>7.7266</b>	<b>7.7266</b>	<b>7.7266</b>	<b>7.7266</b>	<b>7.7266</b>	<b>7.7266</b>	<b>7.7266</b>	<b>7.7266</b>	<b>7.7266</b>
m=1, n=1; a/h=5												
	N=1	N=2	N=3	N=4	N=5	N=6	N=7	N=8	N=9	N=10	N=11	N=12
M=3	1.0789	2.2807	1.5681	1.5815	1.5788	1.5788	1.5788	1.5781	<b>1.5788</b>	<b>1.5788</b>	<b>1.5788</b>	<b>1.5788</b>
M=10	1.4693	1.7798	1.5781	1.5790	<b>1.5788</b>	<b>1.5788</b>	<b>1.5788</b>	<b>1.5788</b>	<b>1.5788</b>	<b>1.5788</b>	<b>1.5788</b>	<b>1.5788</b>
M=20	1.5523	1.6313	<b>1.5788</b>	<b>1.5788</b>	<b>1.5788</b>	<b>1.5788</b>	<b>1.5788</b>	<b>1.5788</b>	<b>1.5788</b>	<b>1.5788</b>	<b>1.5788</b>	<b>1.5788</b>
M=40	1.5722	1.5921	<b>1.5788</b>	<b>1.5788</b>	<b>1.5788</b>	<b>1.5788</b>	<b>1.5788</b>	<b>1.5788</b>	<b>1.5788</b>	<b>1.5788</b>	<b>1.5788</b>	<b>1.5788</b>
M=60	1.5759	1.5847	<b>1.5788</b>	<b>1.5788</b>	<b>1.5788</b>	<b>1.5788</b>	<b>1.5788</b>	<b>1.5788</b>	<b>1.5788</b>	<b>1.5788</b>	<b>1.5788</b>	<b>1.5788</b>
M=80	1.5772	1.5821	<b>1.5788</b>	<b>1.5788</b>	<b>1.5788</b>	<b>1.5788</b>	<b>1.5788</b>	<b>1.5788</b>	<b>1.5788</b>	<b>1.5788</b>	<b>1.5788</b>	<b>1.5788</b>
M=100	1.5778	1.5809	<b>1.5788</b>	<b>1.5788</b>	<b>1.5788</b>	<b>1.5788</b>	<b>1.5788</b>	<b>1.5788</b>	<b>1.5788</b>	<b>1.5788</b>	<b>1.5788</b>	<b>1.5788</b>
m=2, n=2; a/h=100												
	N=1	N=2	N=3	N=4	N=5	N=6	N=7	N=8	N=9	N=10	N=11	N=12
M=3	32.563	33.621	<b>32.930</b>	<b>32.930</b>	<b>32.930</b>	<b>32.930</b>	<b>32.930</b>	<b>32.930</b>	<b>32.930</b>	<b>32.930</b>	<b>32.930</b>	<b>32.930</b>
M=10	32.845	33.099	<b>32.930</b>	<b>32.930</b>	<b>32.930</b>	<b>32.930</b>	<b>32.930</b>	<b>32.930</b>	<b>32.930</b>	<b>32.930</b>	<b>32.930</b>	<b>32.930</b>
M=20	32.909	32.972	<b>32.930</b>	<b>32.930</b>	<b>32.930</b>	<b>32.930</b>	<b>32.930</b>	<b>32.930</b>	<b>32.930</b>	<b>32.930</b>	<b>32.930</b>	<b>32.930</b>
M=40	32.925	32.940	<b>32.930</b>	<b>32.930</b>	<b>32.930</b>	<b>32.930</b>	<b>32.930</b>	<b>32.930</b>	<b>32.930</b>	<b>32.930</b>	<b>32.930</b>	<b>32.930</b>
M=60	32.927	32.935	<b>32.930</b>	<b>32.930</b>	<b>32.930</b>	<b>32.930</b>	<b>32.930</b>	<b>32.930</b>	<b>32.930</b>	<b>32.930</b>	<b>32.930</b>	<b>32.930</b>
M=80	32.929	32.932	<b>32.930</b>	<b>32.930</b>	<b>32.930</b>	<b>32.930</b>	<b>32.930</b>	<b>32.930</b>	<b>32.930</b>	<b>32.930</b>	<b>32.930</b>	<b>32.930</b>
M=100	32.929	32.932	<b>32.930</b>	<b>32.930</b>	<b>32.930</b>	<b>32.930</b>	<b>32.930</b>	<b>32.930</b>	<b>32.930</b>	<b>32.930</b>	<b>32.930</b>	<b>32.930</b>
m=2, n=2; a/h=5												
	N=1	N=2	N=3	N=4	N=5	N=6	N=7	N=8	N=9	N=10	N=11	N=12
M=3	2.3138	8.2012	4.8647	5.1199	5.0664	5.0679	<b>5.0677</b>	<b>5.0677</b>	<b>5.0677</b>	<b>5.0677</b>	<b>5.0677</b>	<b>5.0677</b>
M=10	4.5654	5.9848	5.0553	5.0708	<b>5.0677</b>	<b>5.0677</b>	<b>5.0677</b>	<b>5.0677</b>	<b>5.0677</b>	<b>5.0677</b>	<b>5.0677</b>	<b>5.0677</b>
M=20	4.9495	5.3100	5.0669	5.0679	<b>5.0677</b>	<b>5.0677</b>	<b>5.0677</b>	<b>5.0677</b>	<b>5.0677</b>	<b>5.0677</b>	<b>5.0677</b>	<b>5.0677</b>
M=40	5.0386	5.1292	<b>5.0677</b>	<b>5.0677</b>	<b>5.0677</b>	<b>5.0677</b>	<b>5.0677</b>	<b>5.0677</b>	<b>5.0677</b>	<b>5.0677</b>	<b>5.0677</b>	<b>5.0677</b>
M=60	5.0548	5.0951	<b>5.0677</b>	<b>5.0677</b>	<b>5.0677</b>	<b>5.0677</b>	<b>5.0677</b>	<b>5.0677</b>	<b>5.0677</b>	<b>5.0677</b>	<b>5.0677</b>	<b>5.0677</b>
M=80	5.0604	5.0831	<b>5.0677</b>	<b>5.0677</b>	<b>5.0677</b>	<b>5.0677</b>	<b>5.0677</b>	<b>5.0677</b>	<b>5.0677</b>	<b>5.0677</b>	<b>5.0677</b>	<b>5.0677</b>
M=100	5.0631	5.0676	<b>5.0677</b>	<b>5.0677</b>	<b>5.0677</b>	<b>5.0677</b>	<b>5.0677</b>	<b>5.0677</b>	<b>5.0677</b>	<b>5.0677</b>	<b>5.0677</b>	<b>5.0677</b>

Table 5: Sandwich plate with isotropic skins. First mode (I) given as dimensionless circular frequency  $\bar{\omega} = \omega(a^2/h)\sqrt{\rho_{skin}/E_{skin}}$ . Three physical layers ( $N_L=3$ ) divided in M mathematical layers.

m=1, n=1; R <sub>α</sub> /h=100												
	N=1	N=2	N=3	N=4	N=5	N=6	N=7	N=8	N=9	N=10	N=11	N=12
M=3	20.633	22.454	22.433	22.433	22.433	22.433	22.433	22.431	22.433	22.433	22.433	22.433
M=10	21.562	22.437	<b>22.432</b>	<b>22.432</b>	<b>22.432</b>	<b>22.432</b>	<b>22.432</b>	<b>22.432</b>	<b>22.432</b>	<b>22.432</b>	<b>22.432</b>	<b>22.432</b>
M=20	22.002	22.433	<b>22.432</b>	<b>22.432</b>	<b>22.432</b>	<b>22.432</b>	<b>22.432</b>	<b>22.432</b>	<b>22.432</b>	<b>22.432</b>	<b>22.432</b>	<b>22.432</b>
M=40	22.218	<b>22.432</b>	<b>22.432</b>	<b>22.432</b>	<b>22.432</b>	<b>22.432</b>	<b>22.432</b>	<b>22.432</b>	<b>22.432</b>	<b>22.432</b>	<b>22.432</b>	<b>22.432</b>
M=60	22.289	<b>22.432</b>	<b>22.432</b>	<b>22.432</b>	<b>22.432</b>	<b>22.432</b>	<b>22.432</b>	<b>22.432</b>	<b>22.432</b>	<b>22.432</b>	<b>22.432</b>	<b>22.432</b>
M=80	22.325	<b>22.432</b>	<b>22.432</b>	<b>22.432</b>	<b>22.432</b>	<b>22.432</b>	<b>22.432</b>	<b>22.432</b>	<b>22.432</b>	<b>22.432</b>	<b>22.432</b>	<b>22.432</b>
M=100	22.346	<b>22.432</b>	<b>22.432</b>	<b>22.432</b>	<b>22.432</b>	<b>22.432</b>	<b>22.432</b>	<b>22.432</b>	<b>22.432</b>	<b>22.432</b>	<b>22.432</b>	<b>22.432</b>
m=1, n=1; R <sub>α</sub> /h=5												
	N=1	N=2	N=3	N=4	N=5	N=6	N=7	N=8	N=9	N=10	N=11	N=12
M=3	6.4503	1.8102	0.0001	0.0000	339.24	339.58	339.58	339.58	1.4981	1.4981	1.4981	1.4981
M=10	0.0014	339.58	1.4831	1.4848	1.4847	1.4847	1.4847	1.4847	1.4847	1.4847	1.4847	1.4847
M=20	339.58	1.5013	1.4809	1.4811	1.4811	1.4811	1.4811	1.4811	1.4811	1.4811	1.4811	1.4811
M=40	1.3044	1.4852	1.4802	1.4802	1.4802	1.4802	1.4802	1.4802	1.4802	1.4802	1.4802	1.4802
M=60	1.3660	1.4822	1.4800	1.4800	1.4800	1.4800	1.4800	1.4800	1.4800	1.4800	1.4800	1.4800
M=80	1.3956	1.4812	1.4800	1.4800	1.4800	1.4800	1.4800	1.4800	1.4800	1.4800	1.4800	1.4800
M=100	1.4129	1.4807	<b>1.4799</b>	<b>1.4799</b>	<b>1.4799</b>	<b>1.4799</b>	<b>1.4799</b>	<b>1.4799</b>	<b>1.4799</b>	<b>1.4799</b>	<b>1.4799</b>	<b>1.4799</b>
m=2, n=2; R <sub>α</sub> /h=100												
	N=1	N=2	N=3	N=4	N=5	N=6	N=7	N=8	N=9	N=10	N=11	N=12
M=3	21.124	29.205	28.902	28.903	28.903	28.903	28.903	28.903	28.903	28.903	28.903	28.903
M=10	25.375	28.973	28.899	28.899	28.899	28.899	28.899	28.899	28.899	28.899	28.899	28.899
M=20	27.203	28.917	<b>28.898</b>	<b>28.898</b>	<b>28.898</b>	<b>28.898</b>	<b>28.898</b>	<b>28.898</b>	<b>28.898</b>	<b>28.898</b>	<b>28.898</b>	<b>28.898</b>
M=40	28.066	28.902	<b>28.898</b>	<b>28.898</b>	<b>28.898</b>	<b>28.898</b>	<b>28.898</b>	<b>28.898</b>	<b>28.898</b>	<b>28.898</b>	<b>28.898</b>	<b>28.898</b>
M=60	28.346	28.900	<b>28.898</b>	<b>28.898</b>	<b>28.898</b>	<b>28.898</b>	<b>28.898</b>	<b>28.898</b>	<b>28.898</b>	<b>28.898</b>	<b>28.898</b>	<b>28.898</b>
M=80	28.485	28.899	<b>28.898</b>	<b>28.898</b>	<b>28.898</b>	<b>28.898</b>	<b>28.898</b>	<b>28.898</b>	<b>28.898</b>	<b>28.898</b>	<b>28.898</b>	<b>28.898</b>
M=100	28.568	<b>28.898</b>	<b>28.898</b>	<b>28.898</b>	<b>28.898</b>	<b>28.898</b>	<b>28.898</b>	<b>28.898</b>	<b>28.898</b>	<b>28.898</b>	<b>28.898</b>	<b>28.898</b>
m=2, n=2; R <sub>α</sub> /h=5												
	N=1	N=2	N=3	N=4	N=5	N=6	N=7	N=8	N=9	N=10	N=11	N=12
M=3	4.5473	5.4610	69.937	0.0003	340.24	339.58	339.58	339.58	3.5679	3.5679	3.5679	3.5679
M=10	72.747	339.58	3.5287	3.5447	3.5435	3.5435	3.5435	3.5435	3.5435	3.5435	3.5435	3.5435
M=20	339.58	3.6813	3.5351	3.5367	3.5366	3.5366	3.5366	3.5366	3.5366	3.5366	3.5366	3.5366
M=40	3.1762	3.5712	3.5347	3.5349	3.5349	3.5349	3.5349	3.5349	3.5349	3.5349	3.5349	3.5349
M=60	3.3043	3.5507	3.5345	3.5346	3.5346	3.5346	3.5346	3.5346	3.5346	3.5346	3.5346	3.5346
M=80	3.3649	3.5435	3.5344	3.5345	3.5345	3.5345	3.5345	3.5345	3.5345	3.5345	3.5345	3.5345
M=100	3.4002	3.5402	<b>3.5344</b>	<b>3.5344</b>	<b>3.5344</b>	<b>3.5344</b>	<b>3.5344</b>	<b>3.5344</b>	<b>3.5344</b>	<b>3.5344</b>	<b>3.5344</b>	<b>3.5344</b>

Table 6: Sandwich cylindrical shell with isotropic skins. First mode (I) given as dimensionless circular frequency  $\bar{\omega} = \omega(a^2/h)\sqrt{\rho_{skin}/E_{skin}}$ . Three physical layers (N<sub>L</sub>=3) divided in M mathematical layers.

m=2, n=1; R <sub>α</sub> /h=100												
	N=1	N=2	N=3	N=4	N=5	N=6	N=7	N=8	N=9	N=10	N=11	N=12
M=5	464.05	<b>463.99</b>	<b>463.99</b>	<b>463.99</b>	<b>463.99</b>	<b>463.99</b>	<b>463.99</b>	<b>463.99</b>	<b>463.99</b>	<b>463.99</b>	<b>463.99</b>	<b>463.99</b>
M=10	464.05	<b>463.99</b>	<b>463.99</b>	<b>463.99</b>	<b>463.99</b>	<b>463.99</b>	<b>463.99</b>	<b>463.99</b>	<b>463.99</b>	<b>463.99</b>	<b>463.99</b>	<b>463.99</b>
M=20	464.02	<b>463.99</b>	<b>463.99</b>	<b>463.99</b>	<b>463.99</b>	<b>463.99</b>	<b>463.99</b>	<b>463.99</b>	<b>463.99</b>	<b>463.99</b>	<b>463.99</b>	<b>463.99</b>
M=40	464.00	<b>463.99</b>	<b>463.99</b>	<b>463.99</b>	<b>463.99</b>	<b>463.99</b>	<b>463.99</b>	<b>463.99</b>	<b>463.99</b>	<b>463.99</b>	<b>463.99</b>	<b>463.99</b>
M=60	464.00	<b>463.99</b>	<b>463.99</b>	<b>463.99</b>	<b>463.99</b>	<b>463.99</b>	<b>463.99</b>	<b>463.99</b>	<b>463.99</b>	<b>463.99</b>	<b>463.99</b>	<b>463.99</b>
M=80	464.00	<b>463.99</b>	<b>463.99</b>	<b>463.99</b>	<b>463.99</b>	<b>463.99</b>	<b>463.99</b>	<b>463.99</b>	<b>463.99</b>	<b>463.99</b>	<b>463.99</b>	<b>463.99</b>
M=100	<b>463.99</b>	<b>463.99</b>	<b>463.99</b>	<b>463.99</b>	<b>463.99</b>	<b>463.99</b>	<b>463.99</b>	<b>463.99</b>	<b>463.99</b>	<b>463.99</b>	<b>463.99</b>	<b>463.99</b>
m=2, n=1; R <sub>α</sub> /h=5												
	N=1	N=2	N=3	N=4	N=5	N=6	N=7	N=8	N=9	N=10	N=11	N=12
M=5	23.462	8027.3	22263	24075	<b>23.404</b>	<b>23.404</b>	<b>23.404</b>	<b>23.404</b>	<b>23.404</b>	<b>23.404</b>	<b>23.404</b>	<b>23.404</b>
M=10	0.0079	24075	<b>23.404</b>	<b>23.404</b>	<b>23.404</b>	<b>23.404</b>	<b>23.404</b>	<b>23.404</b>	<b>23.404</b>	<b>23.404</b>	<b>23.404</b>	<b>23.404</b>
M=20	24075	23.405	<b>23.404</b>	<b>23.404</b>	<b>23.404</b>	<b>23.404</b>	<b>23.404</b>	<b>23.404</b>	<b>23.404</b>	<b>23.404</b>	<b>23.404</b>	<b>23.404</b>
M=40	23.420	<b>23.404</b>	<b>23.404</b>	<b>23.404</b>	<b>23.404</b>	<b>23.404</b>	<b>23.404</b>	<b>23.404</b>	<b>23.404</b>	<b>23.404</b>	<b>23.404</b>	<b>23.404</b>
M=60	23.415	<b>23.404</b>	<b>23.404</b>	<b>23.404</b>	<b>23.404</b>	<b>23.404</b>	<b>23.404</b>	<b>23.404</b>	<b>23.404</b>	<b>23.404</b>	<b>23.404</b>	<b>23.404</b>
M=80	23.412	<b>23.404</b>	<b>23.404</b>	<b>23.404</b>	<b>23.404</b>	<b>23.404</b>	<b>23.404</b>	<b>23.404</b>	<b>23.404</b>	<b>23.404</b>	<b>23.404</b>	<b>23.404</b>
M=100	23.410	<b>23.404</b>	<b>23.404</b>	<b>23.404</b>	<b>23.404</b>	<b>23.404</b>	<b>23.404</b>	<b>23.404</b>	<b>23.404</b>	<b>23.404</b>	<b>23.404</b>	<b>23.404</b>
m=2, n=3; R <sub>α</sub> /h=100												
	N=1	N=2	N=3	N=4	N=5	N=6	N=7	N=8	N=9	N=10	N=11	N=12
M=5	<b>1786.6</b>	<b>1786.6</b>	<b>1786.6</b>	<b>1786.6</b>	<b>1786.6</b>	<b>1786.6</b>	<b>1786.6</b>	<b>1786.6</b>	<b>1786.6</b>	<b>1786.6</b>	<b>1786.6</b>	<b>1786.6</b>
M=10	1786.7	<b>1786.6</b>	<b>1786.6</b>	<b>1786.6</b>	<b>1786.6</b>	<b>1786.6</b>	<b>1786.6</b>	<b>1786.6</b>	<b>1786.6</b>	<b>1786.6</b>	<b>1786.6</b>	<b>1786.6</b>
M=20	<b>1786.6</b>	<b>1786.6</b>	<b>1786.6</b>	<b>1786.6</b>	<b>1786.6</b>	<b>1786.6</b>	<b>1786.6</b>	<b>1786.6</b>	<b>1786.6</b>	<b>1786.6</b>	<b>1786.6</b>	<b>1786.6</b>
M=40	<b>1786.6</b>	<b>1786.6</b>	<b>1786.6</b>	<b>1786.6</b>	<b>1786.6</b>	<b>1786.6</b>	<b>1786.6</b>	<b>1786.6</b>	<b>1786.6</b>	<b>1786.6</b>	<b>1786.6</b>	<b>1786.6</b>
M=60	<b>1786.6</b>	<b>1786.6</b>	<b>1786.6</b>	<b>1786.6</b>	<b>1786.6</b>	<b>1786.6</b>	<b>1786.6</b>	<b>1786.6</b>	<b>1786.6</b>	<b>1786.6</b>	<b>1786.6</b>	<b>1786.6</b>
M=80	<b>1786.6</b>	<b>1786.6</b>	<b>1786.6</b>	<b>1786.6</b>	<b>1786.6</b>	<b>1786.6</b>	<b>1786.6</b>	<b>1786.6</b>	<b>1786.6</b>	<b>1786.6</b>	<b>1786.6</b>	<b>1786.6</b>
M=100	<b>1786.6</b>	<b>1786.6</b>	<b>1786.6</b>	<b>1786.6</b>	<b>1786.6</b>	<b>1786.6</b>	<b>1786.6</b>	<b>1786.6</b>	<b>1786.6</b>	<b>1786.6</b>	<b>1786.6</b>	<b>1786.6</b>
m=2, n=3; R <sub>α</sub> /h=5												
	N=1	N=2	N=3	N=4	N=5	N=6	N=7	N=8	N=9	N=10	N=11	N=12
M=5	90.350	8020.1	26587	24075	90.348	90.348	90.348	90.348	90.348	90.348	90.348	90.348
M=10	5554.8	24075	90.349	90.349	90.349	90.349	90.349	90.349	90.349	90.349	90.349	90.349
M=20	24075	90.360	90.350	90.350	90.350	90.350	90.350	90.350	90.350	90.350	90.350	90.350
M=40	90.360	90.353	90.350	90.350	90.350	90.350	90.350	90.350	90.350	90.350	90.350	90.350
M=60	90.357	90.352	<b>90.351</b>	<b>90.351</b>	<b>90.351</b>	<b>90.351</b>	<b>90.351</b>	<b>90.351</b>	<b>90.351</b>	<b>90.351</b>	<b>90.351</b>	<b>90.351</b>
M=80	90.355	<b>90.351</b>	<b>90.351</b>	<b>90.351</b>	<b>90.351</b>	<b>90.351</b>	<b>90.351</b>	<b>90.351</b>	<b>90.351</b>	<b>90.351</b>	<b>90.351</b>	<b>90.351</b>
M=100	90.354	<b>90.351</b>	<b>90.351</b>	<b>90.351</b>	<b>90.351</b>	<b>90.351</b>	<b>90.351</b>	<b>90.351</b>	<b>90.351</b>	<b>90.351</b>	<b>90.351</b>	<b>90.351</b>

Table 7: Sandwich cylinder with composite skins. First mode (I) given as dimensionless circular frequency  $\bar{\omega} = \omega(a^2/h)\sqrt{\rho_{skin}/E_{2skin}}$ . Five physical layers (N<sub>L</sub>=5) divided in M mathematical layers.

m=1, n=1; R <sub>α</sub> /h=100												
	N=1	N=2	N=3	N=4	N=5	N=6	N=7	N=8	N=9	N=10	N=11	N=12
M=5	135.15	135.46	<b>135.45</b>	<b>135.45</b>	<b>135.45</b>	<b>135.45</b>	<b>135.45</b>	<b>135.45</b>	<b>135.45</b>	<b>135.45</b>	<b>135.45</b>	<b>135.45</b>
M=10	135.20	<b>135.45</b>	<b>135.45</b>	<b>135.45</b>	<b>135.45</b>	<b>135.45</b>	<b>135.45</b>	<b>135.45</b>	<b>135.45</b>	<b>135.45</b>	<b>135.45</b>	<b>135.45</b>
M=20	135.33	<b>135.45</b>	<b>135.45</b>	<b>135.45</b>	<b>135.45</b>	<b>135.45</b>	<b>135.45</b>	<b>135.45</b>	<b>135.45</b>	<b>135.45</b>	<b>135.45</b>	<b>135.45</b>
M=40	135.39	<b>135.45</b>	<b>135.45</b>	<b>135.45</b>	<b>135.45</b>	<b>135.45</b>	<b>135.45</b>	<b>135.45</b>	<b>135.45</b>	<b>135.45</b>	<b>135.45</b>	<b>135.45</b>
M=60	135.41	<b>135.45</b>	<b>135.45</b>	<b>135.45</b>	<b>135.45</b>	<b>135.45</b>	<b>135.45</b>	<b>135.45</b>	<b>135.45</b>	<b>135.45</b>	<b>135.45</b>	<b>135.45</b>
M=80	135.42	<b>135.45</b>	<b>135.45</b>	<b>135.45</b>	<b>135.45</b>	<b>135.45</b>	<b>135.45</b>	<b>135.45</b>	<b>135.45</b>	<b>135.45</b>	<b>135.45</b>	<b>135.45</b>
M=100	135.42	<b>135.45</b>	<b>135.45</b>	<b>135.45</b>	<b>135.45</b>	<b>135.45</b>	<b>135.45</b>	<b>135.45</b>	<b>135.45</b>	<b>135.45</b>	<b>135.45</b>	<b>135.45</b>
m=1, n=1; R <sub>α</sub> /h=5												
	N=1	N=2	N=3	N=4	N=5	N=6	N=7	N=8	N=9	N=10	N=11	N=12
M=5	7.0083	226.32	0.0000	668.75	7.2408	7.2408	7.2408	7.2408	7.2408	7.2408	7.2408	7.2408
M=10	148.16	668.75	7.2379	7.2443	7.2436	7.2437	7.2437	7.2437	7.2437	7.2437	7.2437	7.2437
M=20	668.75	7.2725	7.2422	7.2429	7.2428	7.2428	7.2428	7.2428	7.2428	7.2428	7.2428	7.2428
M=40	7.1867	7.2498	7.2425	7.2426	7.2426	7.2426	7.2426	7.2426	7.2426	7.2426	7.2426	7.2426
M=60	7.2061	7.2458	7.2426	7.2426	7.2426	7.2426	7.2426	7.2426	7.2426	7.2426	7.2426	7.2426
M=80	7.2155	7.2443	7.2425	7.2426	7.2426	7.2426	7.2426	7.2426	7.2426	7.2426	7.2426	7.2426
M=100	7.2211	7.2437	<b>7.2425</b>	<b>7.2425</b>	<b>7.2425</b>	<b>7.2425</b>	<b>7.2425</b>	<b>7.2425</b>	<b>7.2425</b>	<b>7.2425</b>	<b>7.2425</b>	<b>7.2425</b>
m=2, n=2; R <sub>α</sub> /h=100												
	N=1	N=2	N=3	N=4	N=5	N=6	N=7	N=8	N=9	N=10	N=11	N=12
M=5	150.91	152.39	<b>152.25</b>	<b>152.25</b>	<b>152.25</b>	<b>152.25</b>	<b>152.25</b>	<b>152.25</b>	<b>152.25</b>	<b>152.25</b>	<b>152.25</b>	<b>152.25</b>
M=10	151.05	152.37	<b>152.25</b>	<b>152.25</b>	<b>152.25</b>	<b>152.25</b>	<b>152.25</b>	<b>152.25</b>	<b>152.25</b>	<b>152.25</b>	<b>152.25</b>	<b>152.25</b>
M=20	151.66	152.28	<b>152.25</b>	<b>152.25</b>	<b>152.25</b>	<b>152.25</b>	<b>152.25</b>	<b>152.25</b>	<b>152.25</b>	<b>152.25</b>	<b>152.25</b>	<b>152.25</b>
M=40	151.96	152.26	<b>152.25</b>	<b>152.25</b>	<b>152.25</b>	<b>152.25</b>	<b>152.25</b>	<b>152.25</b>	<b>152.25</b>	<b>152.25</b>	<b>152.25</b>	<b>152.25</b>
M=60	152.06	<b>152.25</b>	<b>152.25</b>	<b>152.25</b>	<b>152.25</b>	<b>152.25</b>	<b>152.25</b>	<b>152.25</b>	<b>152.25</b>	<b>152.25</b>	<b>152.25</b>	<b>152.25</b>
M=80	152.11	<b>152.25</b>	<b>152.25</b>	<b>152.25</b>	<b>152.25</b>	<b>152.25</b>	<b>152.25</b>	<b>152.25</b>	<b>152.25</b>	<b>152.25</b>	<b>152.25</b>	<b>152.25</b>
M=100	152.14	<b>152.25</b>	<b>152.25</b>	<b>152.25</b>	<b>152.25</b>	<b>152.25</b>	<b>152.25</b>	<b>152.25</b>	<b>152.25</b>	<b>152.25</b>	<b>152.25</b>	<b>152.25</b>
m=2, n=2; R <sub>α</sub> /h=5												
	N=1	N=2	N=3	N=4	N=5	N=6	N=7	N=8	N=9	N=10	N=11	N=12
M=5	9.5926	8.8982	660.27	668.75	10.687	10.687	10.687	10.687	10.687	10.687	10.687	10.687
M=10	4.6405	668.75	10.554	10.727	10.696	10.698	10.698	10.698	10.698	10.698	10.698	10.698
M=20	668.75	11.062	10.684	10.696	10.695	10.695	10.695	10.695	10.695	10.695	10.695	10.695
M=40	10.483	10.784	10.693	<b>10.694</b>	<b>10.694</b>	<b>10.694</b>	<b>10.694</b>	<b>10.694</b>	<b>10.694</b>	<b>10.694</b>	<b>10.694</b>	<b>10.694</b>
M=60	10.563	10.733	<b>10.694</b>	<b>10.694</b>	<b>10.694</b>	<b>10.694</b>	<b>10.694</b>	<b>10.694</b>	<b>10.694</b>	<b>10.694</b>	<b>10.694</b>	<b>10.694</b>
M=80	10.599	10.716	<b>10.694</b>	<b>10.694</b>	<b>10.694</b>	<b>10.694</b>	<b>10.694</b>	<b>10.694</b>	<b>10.694</b>	<b>10.694</b>	<b>10.694</b>	<b>10.694</b>
M=100	10.620	10.708	<b>10.694</b>	<b>10.694</b>	<b>10.694</b>	<b>10.694</b>	<b>10.694</b>	<b>10.694</b>	<b>10.694</b>	<b>10.694</b>	<b>10.694</b>	<b>10.694</b>

Table 8: Sandwich spherical shell with composite skins. First mode (I) given as dimensionless circular frequency  $\bar{\omega} = \omega(a^2/h)\sqrt{\rho_{skin}/E_{2skin}}$ . Five physical layers (N<sub>L</sub>=5) divided in M mathematical layers.



m=1, n=1; I mode												
	N=1	N=2	N=3	N=4	N=5	N=6	N=7	N=8	N=9	N=10	N=11	N=12
M=3	1.0789	2.2807	1.5681	1.5815	1.5788	1.5788	1.5788	1.5781	<b>1.5788</b>	<b>1.5788</b>	<b>1.5788</b>	<b>1.5788</b>
M=10	1.4693	1.7798	1.5781	1.5790	<b>1.5788</b>	<b>1.5788</b>	<b>1.5788</b>	<b>1.5788</b>	<b>1.5788</b>	<b>1.5788</b>	<b>1.5788</b>	<b>1.5788</b>
M=20	1.5523	1.6313	<b>1.5788</b>	<b>1.5788</b>	<b>1.5788</b>	<b>1.5788</b>	<b>1.5788</b>	<b>1.5788</b>	<b>1.5788</b>	<b>1.5788</b>	<b>1.5788</b>	<b>1.5788</b>
M=40	1.5722	1.5921	<b>1.5788</b>	<b>1.5788</b>	<b>1.5788</b>	<b>1.5788</b>	<b>1.5788</b>	<b>1.5788</b>	<b>1.5788</b>	<b>1.5788</b>	<b>1.5788</b>	<b>1.5788</b>
M=60	1.5759	1.5847	<b>1.5788</b>	<b>1.5788</b>	<b>1.5788</b>	<b>1.5788</b>	<b>1.5788</b>	<b>1.5788</b>	<b>1.5788</b>	<b>1.5788</b>	<b>1.5788</b>	<b>1.5788</b>
M=80	1.5772	1.5821	<b>1.5788</b>	<b>1.5788</b>	<b>1.5788</b>	<b>1.5788</b>	<b>1.5788</b>	<b>1.5788</b>	<b>1.5788</b>	<b>1.5788</b>	<b>1.5788</b>	<b>1.5788</b>
M=100	1.5778	1.5809	<b>1.5788</b>	<b>1.5788</b>	<b>1.5788</b>	<b>1.5788</b>	<b>1.5788</b>	<b>1.5788</b>	<b>1.5788</b>	<b>1.5788</b>	<b>1.5788</b>	<b>1.5788</b>
m=1, n=1; II mode												
	N=1	N=2	N=3	N=4	N=5	N=6	N=7	N=8	N=9	N=10	N=11	N=12
M=3	6.5600	6.3041	6.4856	6.4941	6.4927	6.4925	6.4925	6.4980	<b>6.4925</b>	<b>6.4925</b>	<b>6.4925</b>	<b>6.4925</b>
M=10	6.4670	6.5260	6.4924	6.4926	<b>6.4925</b>	<b>6.4925</b>	<b>6.4925</b>	<b>6.4925</b>	<b>6.4925</b>	<b>6.4925</b>	<b>6.4925</b>	<b>6.4925</b>
M=20	6.4862	6.5009	<b>6.4925</b>	<b>6.4925</b>	<b>6.4925</b>	<b>6.4925</b>	<b>6.4925</b>	<b>6.4925</b>	<b>6.4925</b>	<b>6.4925</b>	<b>6.4925</b>	<b>6.4925</b>
M=40	6.4910	6.4946	<b>6.4925</b>	<b>6.4925</b>	<b>6.4925</b>	<b>6.4925</b>	<b>6.4925</b>	<b>6.4925</b>	<b>6.4925</b>	<b>6.4925</b>	<b>6.4925</b>	<b>6.4925</b>
M=60	6.4918	6.4935	<b>6.4925</b>	<b>6.4925</b>	<b>6.4925</b>	<b>6.4925</b>	<b>6.4925</b>	<b>6.4925</b>	<b>6.4925</b>	<b>6.4925</b>	<b>6.4925</b>	<b>6.4925</b>
M=80	6.4922	6.4931	<b>6.4925</b>	<b>6.4925</b>	<b>6.4925</b>	<b>6.4925</b>	<b>6.4925</b>	<b>6.4925</b>	<b>6.4925</b>	<b>6.4925</b>	<b>6.4925</b>	<b>6.4925</b>
M=100	6.4923	6.4929	<b>6.4925</b>	<b>6.4925</b>	<b>6.4925</b>	<b>6.4925</b>	<b>6.4925</b>	<b>6.4925</b>	<b>6.4925</b>	<b>6.4925</b>	<b>6.4925</b>	<b>6.4925</b>
m=1, n=1; III mode												
	N=1	N=2	N=3	N=4	N=5	N=6	N=7	N=8	N=9	N=10	N=11	N=12
M=3	13.659	13.561	13.567	13.594	13.592	13.591	13.591	13.539	<b>13.591</b>	<b>13.591</b>	<b>13.591</b>	<b>13.591</b>
M=10	13.595	13.589	<b>13.591</b>	<b>13.591</b>	<b>13.591</b>	<b>13.591</b>	<b>13.591</b>	<b>13.591</b>	<b>13.591</b>	<b>13.591</b>	<b>13.591</b>	<b>13.591</b>
M=20	13.592	<b>13.591</b>	<b>13.591</b>	<b>13.591</b>	<b>13.591</b>	<b>13.591</b>	<b>13.591</b>	<b>13.591</b>	<b>13.591</b>	<b>13.591</b>	<b>13.591</b>	<b>13.591</b>
M=40	<b>13.591</b>	<b>13.591</b>	<b>13.591</b>	<b>13.591</b>	<b>13.591</b>	<b>13.591</b>	<b>13.591</b>	<b>13.591</b>	<b>13.591</b>	<b>13.591</b>	<b>13.591</b>	<b>13.591</b>
M=60	<b>13.591</b>	<b>13.591</b>	<b>13.591</b>	<b>13.591</b>	<b>13.591</b>	<b>13.591</b>	<b>13.591</b>	<b>13.591</b>	<b>13.591</b>	<b>13.591</b>	<b>13.591</b>	<b>13.591</b>
M=80	<b>13.591</b>	<b>13.591</b>	<b>13.591</b>	<b>13.591</b>	<b>13.591</b>	<b>13.591</b>	<b>13.591</b>	<b>13.591</b>	<b>13.591</b>	<b>13.591</b>	<b>13.591</b>	<b>13.591</b>
M=100	<b>13.591</b>	<b>13.591</b>	<b>13.591</b>	<b>13.591</b>	<b>13.591</b>	<b>13.591</b>	<b>13.591</b>	<b>13.591</b>	<b>13.591</b>	<b>13.591</b>	<b>13.591</b>	<b>13.591</b>
m=1, n=1; IV mode												
	N=1	N=2	N=3	N=4	N=5	N=6	N=7	N=8	N=9	N=10	N=11	N=12
M=3	14.235	14.016	14.018	14.061	14.059	14.056	14.056	14.106	<b>14.056</b>	<b>14.056</b>	<b>14.056</b>	<b>14.056</b>
M=10	14.063	14.053	<b>14.056</b>	<b>14.056</b>	<b>14.056</b>	<b>14.056</b>	<b>14.056</b>	<b>14.056</b>	<b>14.056</b>	<b>14.056</b>	<b>14.056</b>	<b>14.056</b>
M=20	14.058	14.055	<b>14.056</b>	<b>14.056</b>	<b>14.056</b>	<b>14.056</b>	<b>14.056</b>	<b>14.056</b>	<b>14.056</b>	<b>14.056</b>	<b>14.056</b>	<b>14.056</b>
M=40	14.057	<b>14.056</b>	<b>14.056</b>	<b>14.056</b>	<b>14.056</b>	<b>14.056</b>	<b>14.056</b>	<b>14.056</b>	<b>14.056</b>	<b>14.056</b>	<b>14.056</b>	<b>14.056</b>
M=60	<b>14.056</b>	<b>14.056</b>	<b>14.056</b>	<b>14.056</b>	<b>14.056</b>	<b>14.056</b>	<b>14.056</b>	<b>14.056</b>	<b>14.056</b>	<b>14.056</b>	<b>14.056</b>	<b>14.056</b>
M=80	<b>14.056</b>	<b>14.056</b>	<b>14.056</b>	<b>14.056</b>	<b>14.056</b>	<b>14.056</b>	<b>14.056</b>	<b>14.056</b>	<b>14.056</b>	<b>14.056</b>	<b>14.056</b>	<b>14.056</b>
M=100	<b>14.056</b>	<b>14.056</b>	<b>14.056</b>	<b>14.056</b>	<b>14.056</b>	<b>14.056</b>	<b>14.056</b>	<b>14.056</b>	<b>14.056</b>	<b>14.056</b>	<b>14.056</b>	<b>14.056</b>

Table 9: Sandwich plate with isotropic skins and thickness ratio  $a/h=5$ . Modes from I to IV ( $m=n=1$ ) given as dimensionless circular frequency  $\bar{\omega} = \omega(a^2/h)\sqrt{\rho_{skin}/E_{skin}}$ . Three physical layers ( $N_L=3$ ) divided in M mathematical layers.

m=1, n=1; I mode												
	N=1	N=2	N=3	N=4	N=5	N=6	N=7	N=8	N=9	N=10	N=11	N=12
M=3	6.4503	1.8102	0.0001	0.0000	339.65	339.58	339.58	339.58	1.4981	1.4981	1.4981	1.4981
M=10	0.0014	339.58	1.4831	1.4847	1.4847	1.4847	1.4847	1.4847	1.4847	1.4847	1.4847	1.4847
M=20	339.58	1.5013	1.4809	1.4811	1.4811	1.4811	1.4811	1.4811	1.4811	1.4811	1.4811	1.4811
M=40	1.3044	1.4852	1.4802	1.4802	1.4802	1.4802	1.4802	1.4802	1.4802	1.4802	1.4802	1.4802
M=60	1.3660	1.4822	1.4800	1.4800	1.4800	1.4800	1.4800	1.4800	1.4800	1.4800	1.4800	1.4800
M=80	1.3956	1.4812	1.4800	1.4800	1.4800	1.4800	1.4800	1.4800	1.4800	1.4800	1.4800	1.4800
M=100	1.4129	1.4807	<b>1.4799</b>	<b>1.4799</b>	<b>1.4799</b>	<b>1.4799</b>	<b>1.4799</b>	<b>1.4799</b>	<b>1.4799</b>	<b>1.4799</b>	<b>1.4799</b>	<b>1.4799</b>
m=1, n=1; II mode												
	N=1	N=2	N=3	N=4	N=5	N=6	N=7	N=8	N=9	N=10	N=11	N=12
M=3	11.310	6.6200	206.16	1018.2	376.02	416.27	480.24	480.24	6.8843	6.8843	6.8843	6.8843
M=10	48.641	480.25	6.8849	6.8851	6.8851	6.8851	6.8851	6.8851	6.8851	6.8851	6.8851	6.8851
M=20	480.25	6.8857	6.8845	6.8845	6.8845	6.8845	6.8845	6.8845	6.8845	6.8845	6.8845	6.8845
M=40	6.8319	6.8846	<b>6.8843</b>	<b>6.8843</b>	<b>6.8843</b>	<b>6.8843</b>	<b>6.8843</b>	<b>6.8843</b>	<b>6.8843</b>	<b>6.8843</b>	<b>6.8843</b>	<b>6.8843</b>
M=60	6.8495	6.8844	<b>6.8843</b>	<b>6.8843</b>	<b>6.8843</b>	<b>6.8843</b>	<b>6.8843</b>	<b>6.8843</b>	<b>6.8843</b>	<b>6.8843</b>	<b>6.8843</b>	<b>6.8843</b>
M=80	6.8582	6.8844	<b>6.8843</b>	<b>6.8843</b>	<b>6.8843</b>	<b>6.8843</b>	<b>6.8843</b>	<b>6.8843</b>	<b>6.8843</b>	<b>6.8843</b>	<b>6.8843</b>	<b>6.8843</b>
M=100	6.8634	<b>6.8843</b>	<b>6.8843</b>	<b>6.8843</b>	<b>6.8843</b>	<b>6.8843</b>	<b>6.8843</b>	<b>6.8843</b>	<b>6.8843</b>	<b>6.8843</b>	<b>6.8843</b>	<b>6.8843</b>
m=1, n=1; III mode												
	N=1	N=2	N=3	N=4	N=5	N=6	N=7	N=8	N=9	N=10	N=11	N=12
M=3	12.955	11.244	206.79	NaN	NaN	1517.8	588.06	588.34	11.279	11.279	11.279	11.279
M=10	76.612	537.10	<b>11.278</b>	<b>11.278</b>	<b>11.278</b>	<b>11.278</b>	<b>11.278</b>	<b>11.278</b>	<b>11.278</b>	<b>11.278</b>	<b>11.278</b>	<b>11.278</b>
M=20	618.05	<b>11.278</b>	<b>11.278</b>	<b>11.278</b>	<b>11.278</b>	<b>11.278</b>	<b>11.278</b>	<b>11.278</b>	<b>11.278</b>	<b>11.278</b>	<b>11.278</b>	<b>11.278</b>
M=40	11.275	<b>11.278</b>	<b>11.278</b>	<b>11.278</b>	<b>11.278</b>	<b>11.278</b>	<b>11.278</b>	<b>11.278</b>	<b>11.278</b>	<b>11.278</b>	<b>11.278</b>	<b>11.278</b>
M=60	11.276	<b>11.278</b>	<b>11.278</b>	<b>11.278</b>	<b>11.278</b>	<b>11.278</b>	<b>11.278</b>	<b>11.278</b>	<b>11.278</b>	<b>11.278</b>	<b>11.278</b>	<b>11.278</b>
M=80	11.276	<b>11.278</b>	<b>11.278</b>	<b>11.278</b>	<b>11.278</b>	<b>11.278</b>	<b>11.278</b>	<b>11.278</b>	<b>11.278</b>	<b>11.278</b>	<b>11.278</b>	<b>11.278</b>
M=100	11.276	<b>11.278</b>	<b>11.278</b>	<b>11.278</b>	<b>11.278</b>	<b>11.278</b>	<b>11.278</b>	<b>11.278</b>	<b>11.278</b>	<b>11.278</b>	<b>11.278</b>	<b>11.278</b>
m=1, n=1; IV mode												
	N=1	N=2	N=3	N=4	N=5	N=6	N=7	N=8	N=9	N=10	N=11	N=12
M=3	18.963	12.810	NaN	NaN	NaN	NaN	619.90	666.93	<b>12.867</b>	<b>12.867</b>	<b>12.867</b>	<b>12.867</b>
M=10	105.86	6188.4	<b>12.867</b>	<b>12.867</b>	<b>12.867</b>	<b>12.867</b>	<b>12.867</b>	<b>12.867</b>	<b>12.867</b>	<b>12.867</b>	<b>12.867</b>	<b>12.867</b>
M=20	12434	<b>12.867</b>	<b>12.867</b>	<b>12.867</b>	<b>12.867</b>	<b>12.867</b>	<b>12.867</b>	<b>12.867</b>	<b>12.867</b>	<b>12.867</b>	<b>12.867</b>	<b>12.867</b>
M=40	12.863	<b>12.867</b>	<b>12.867</b>	<b>12.867</b>	<b>12.867</b>	<b>12.867</b>	<b>12.867</b>	<b>12.867</b>	<b>12.867</b>	<b>12.867</b>	<b>12.867</b>	<b>12.867</b>
M=60	12.864	<b>12.867</b>	<b>12.867</b>	<b>12.867</b>	<b>12.867</b>	<b>12.867</b>	<b>12.867</b>	<b>12.867</b>	<b>12.867</b>	<b>12.867</b>	<b>12.867</b>	<b>12.867</b>
M=80	12.865	<b>12.867</b>	<b>12.867</b>	<b>12.867</b>	<b>12.867</b>	<b>12.867</b>	<b>12.867</b>	<b>12.867</b>	<b>12.867</b>	<b>12.867</b>	<b>12.867</b>	<b>12.867</b>
M=100	12.865	<b>12.867</b>	<b>12.867</b>	<b>12.867</b>	<b>12.867</b>	<b>12.867</b>	<b>12.867</b>	<b>12.867</b>	<b>12.867</b>	<b>12.867</b>	<b>12.867</b>	<b>12.867</b>

Table 10: Sandwich cylindrical shell with isotropic skins and thickness ratio  $R_\alpha/h=5$ . Modes from I to IV ( $m=n=1$ ) given as dimensionless circular frequency  $\bar{\omega} = \omega(a^2/h)\sqrt{\rho_{skin}/E_{skin}}$ . Three physical layers ( $N_L=3$ ) divided in M mathematical layers.

m=2, n=1; I mode												
	N=1	N=2	N=3	N=4	N=5	N=6	N=7	N=8	N=9	N=10	N=11	N=12
M=5	23.462	8027.3	22263	24075	<b>23.404</b>	<b>23.404</b>	<b>23.404</b>	<b>23.404</b>	<b>23.404</b>	<b>23.404</b>	<b>23.404</b>	<b>23.404</b>
M=10	0.0079	24075	<b>23.404</b>	<b>23.404</b>	<b>23.404</b>	<b>23.404</b>	<b>23.404</b>	<b>23.404</b>	<b>23.404</b>	<b>23.404</b>	<b>23.404</b>	<b>23.404</b>
M=20	24075	23.405	<b>23.404</b>	<b>23.404</b>	<b>23.404</b>	<b>23.404</b>	<b>23.404</b>	<b>23.404</b>	<b>23.404</b>	<b>23.404</b>	<b>23.404</b>	<b>23.404</b>
M=40	23.420	<b>23.404</b>	<b>23.404</b>	<b>23.404</b>	<b>23.404</b>	<b>23.404</b>	<b>23.404</b>	<b>23.404</b>	<b>23.404</b>	<b>23.404</b>	<b>23.404</b>	<b>23.404</b>
M=60	23.415	<b>23.404</b>	<b>23.404</b>	<b>23.404</b>	<b>23.404</b>	<b>23.404</b>	<b>23.404</b>	<b>23.404</b>	<b>23.404</b>	<b>23.404</b>	<b>23.404</b>	<b>23.404</b>
M=80	23.412	<b>23.404</b>	<b>23.404</b>	<b>23.404</b>	<b>23.404</b>	<b>23.404</b>	<b>23.404</b>	<b>23.404</b>	<b>23.404</b>	<b>23.404</b>	<b>23.404</b>	<b>23.404</b>
M=100	23.410	<b>23.404</b>	<b>23.404</b>	<b>23.404</b>	<b>23.404</b>	<b>23.404</b>	<b>23.404</b>	<b>23.404</b>	<b>23.404</b>	<b>23.404</b>	<b>23.404</b>	<b>23.404</b>
m=2, n=1; II mode												
	N=1	N=2	N=3	N=4	N=5	N=6	N=7	N=8	N=9	N=10	N=11	N=12
M=5	211.70	8257.9	22651	24075	211.81	211.81	211.81	211.81	211.81	211.81	211.81	211.81
M=10	3050.8	34026	<b>211.80</b>	<b>211.80</b>	<b>211.80</b>	<b>211.80</b>	<b>211.80</b>	<b>211.80</b>	<b>211.80</b>	<b>211.80</b>	<b>211.80</b>	<b>211.80</b>
M=20	34043	<b>211.80</b>	<b>211.80</b>	<b>211.80</b>	<b>211.80</b>	<b>211.80</b>	<b>211.80</b>	<b>211.80</b>	<b>211.80</b>	<b>211.80</b>	<b>211.80</b>	<b>211.80</b>
M=40	<b>211.80</b>	<b>211.80</b>	<b>211.80</b>	<b>211.80</b>	<b>211.80</b>	<b>211.80</b>	<b>211.80</b>	<b>211.80</b>	<b>211.80</b>	<b>211.80</b>	<b>211.80</b>	<b>211.80</b>
M=60	<b>211.80</b>	<b>211.80</b>	<b>211.80</b>	<b>211.80</b>	<b>211.80</b>	<b>211.80</b>	<b>211.80</b>	<b>211.80</b>	<b>211.80</b>	<b>211.80</b>	<b>211.80</b>	<b>211.80</b>
M=80	<b>211.80</b>	<b>211.80</b>	<b>211.80</b>	<b>211.80</b>	<b>211.80</b>	<b>211.80</b>	<b>211.80</b>	<b>211.80</b>	<b>211.80</b>	<b>211.80</b>	<b>211.80</b>	<b>211.80</b>
M=100	<b>211.80</b>	<b>211.80</b>	<b>211.80</b>	<b>211.80</b>	<b>211.80</b>	<b>211.80</b>	<b>211.80</b>	<b>211.80</b>	<b>211.80</b>	<b>211.80</b>	<b>211.80</b>	<b>211.80</b>
m=2, n=1; III mode												
	N=1	N=2	N=3	N=4	N=5	N=6	N=7	N=8	N=9	N=10	N=11	N=12
M=5	380.76	14181	1553014	37879	378.72	378.72	378.72	378.72	378.72	378.72	378.72	378.72
M=10	5563.1	178895	378.88	378.87	378.87	378.87	378.87	378.87	378.87	378.87	378.87	378.87
M=20	37020	378.83	<b>378.88</b>	<b>378.88</b>	<b>378.88</b>	<b>378.88</b>	<b>378.88</b>	<b>378.88</b>	<b>378.88</b>	<b>378.88</b>	<b>378.88</b>	<b>378.88</b>
M=40	378.25	378.86	<b>378.88</b>	<b>378.88</b>	<b>378.88</b>	<b>378.88</b>	<b>378.88</b>	<b>378.88</b>	<b>378.88</b>	<b>378.88</b>	<b>378.88</b>	<b>378.88</b>
M=60	378.46	378.87	<b>378.88</b>	<b>378.88</b>	<b>378.88</b>	<b>378.88</b>	<b>378.88</b>	<b>378.88</b>	<b>378.88</b>	<b>378.88</b>	<b>378.88</b>	<b>378.88</b>
M=80	378.56	378.87	<b>378.88</b>	<b>378.88</b>	<b>378.88</b>	<b>378.88</b>	<b>378.88</b>	<b>378.88</b>	<b>378.88</b>	<b>378.88</b>	<b>378.88</b>	<b>378.88</b>
M=100	378.62	378.87	<b>378.88</b>	<b>378.88</b>	<b>378.88</b>	<b>378.88</b>	<b>378.88</b>	<b>378.88</b>	<b>378.88</b>	<b>378.88</b>	<b>378.88</b>	<b>378.88</b>
m=2, n=1; IV mode												
	N=1	N=2	N=3	N=4	N=5	N=6	N=7	N=8	N=9	N=10	N=11	N=12
M=5	472.40	15477	NaN	64414	469.61	469.61	469.61	469.61	469.61	469.61	469.61	469.61
M=10	7462.9	NaN	469.79	469.79	469.79	469.79	469.79	469.79	469.79	469.79	469.79	469.79
M=20	69080	469.69	469.79	469.79	469.79	469.79	469.79	469.79	469.79	469.79	469.79	469.79
M=40	468.91	469.76	<b>469.78</b>	<b>469.78</b>	<b>469.78</b>	<b>469.78</b>	<b>469.78</b>	<b>469.78</b>	<b>469.78</b>	<b>469.78</b>	<b>469.78</b>	<b>469.78</b>
M=60	469.19	469.77	<b>469.78</b>	<b>469.78</b>	<b>469.78</b>	<b>469.78</b>	<b>469.78</b>	<b>469.78</b>	<b>469.78</b>	<b>469.78</b>	<b>469.78</b>	<b>469.78</b>
M=80	469.33	469.80	<b>469.78</b>	<b>469.78</b>	<b>469.78</b>	<b>469.78</b>	<b>469.78</b>	<b>469.78</b>	<b>469.78</b>	<b>469.78</b>	<b>469.78</b>	<b>469.78</b>
M=100	469.42	<b>469.78</b>	<b>469.78</b>	<b>469.78</b>	<b>469.78</b>	<b>469.78</b>	<b>469.78</b>	<b>469.78</b>	<b>469.78</b>	<b>469.78</b>	<b>469.78</b>	<b>469.78</b>

Table 11: Sandwich cylinder with composite skins and thickness ratio  $R_\alpha/h=5$ . Modes from I to IV ( $m=2$  and  $n=1$ ) given as dimensionless circular frequency  $\bar{\omega} = \omega(a^2/h)\sqrt{\rho_{skin}/E_{2skin}}$ . Five physical layers ( $N_L=5$ ) divided in M mathematical layers.

m=1, n=1; I mode												
	N=1	N=2	N=3	N=4	N=5	N=6	N=7	N=8	N=9	N=10	N=11	N=12
M=5	7.0083	226.32	0.0000	668.75	7.2408	7.2408	7.2408	7.2408	7.2408	7.2408	7.2408	7.2408
M=10	148.16	668.75	7.2379	7.2443	7.2436	7.2437	7.2437	7.2437	7.2437	7.2437	7.2437	7.2437
M=20	668.75	7.2725	7.2422	7.2429	7.2428	7.2428	7.2428	7.2428	7.2428	7.2428	7.2428	7.2428
M=40	7.1867	7.2498	7.2425	7.2426	7.2426	7.2426	7.2426	7.2426	7.2426	7.2426	7.2426	7.2426
M=60	7.2061	7.2458	7.2426	7.2426	7.2426	7.2426	7.2426	7.2426	7.2426	7.2426	7.2426	7.2426
M=80	7.2155	7.2443	7.2425	7.2426	7.2426	7.2426	7.2426	7.2426	7.2426	7.2426	7.2426	7.2426
M=100	7.2211	7.2437	<b>7.2425</b>	<b>7.2425</b>	<b>7.2425</b>	<b>7.2425</b>	<b>7.2425</b>	<b>7.2425</b>	<b>7.2425</b>	<b>7.2425</b>	<b>7.2425</b>	<b>7.2425</b>
m=1, n=1; II mode												
	N=1	N=2	N=3	N=4	N=5	N=6	N=7	N=8	N=9	N=10	N=11	N=12
M=5	17.950	235.40	51123	945.73	18.376	18.378	18.379	18.379	18.379	18.379	18.379	18.379
M=10	205.44	931.09	18.392	<b>18.393</b>	<b>18.393</b>	<b>18.393</b>	<b>18.393</b>	<b>18.393</b>	<b>18.393</b>	<b>18.393</b>	<b>18.393</b>	<b>18.393</b>
M=20	945.89	18.394	<b>18.393</b>	<b>18.393</b>	<b>18.393</b>	<b>18.393</b>	<b>18.393</b>	<b>18.393</b>	<b>18.393</b>	<b>18.393</b>	<b>18.393</b>	<b>18.393</b>
M=40	18.283	<b>18.393</b>	<b>18.393</b>	<b>18.393</b>	<b>18.393</b>	<b>18.393</b>	<b>18.393</b>	<b>18.393</b>	<b>18.393</b>	<b>18.393</b>	<b>18.393</b>	<b>18.393</b>
M=60	18.320	<b>18.393</b>	<b>18.393</b>	<b>18.393</b>	<b>18.393</b>	<b>18.393</b>	<b>18.393</b>	<b>18.393</b>	<b>18.393</b>	<b>18.393</b>	<b>18.393</b>	<b>18.393</b>
M=80	18.338	<b>18.393</b>	<b>18.393</b>	<b>18.393</b>	<b>18.393</b>	<b>18.393</b>	<b>18.393</b>	<b>18.393</b>	<b>18.393</b>	<b>18.393</b>	<b>18.393</b>	<b>18.393</b>
M=100	18.349	<b>18.393</b>	<b>18.393</b>	<b>18.393</b>	<b>18.393</b>	<b>18.393</b>	<b>18.393</b>	<b>18.393</b>	<b>18.393</b>	<b>18.393</b>	<b>18.393</b>	<b>18.393</b>
m=1, n=1; III mode												
	N=1	N=2	N=3	N=4	N=5	N=6	N=7	N=8	N=9	N=10	N=11	N=12
M=5	38.810	389.74	729.74	1749.8	38.010	37.964	37.967	37.970	37.967	37.969	37.931	37.969
M=10	215.33	4921.2	38.035	38.138	38.047	37.920	37.967	37.965	37.965	37.965	37.965	37.965
M=20	1027.3	37.924	37.963	37.963	37.963	37.963	37.963	37.963	37.963	37.963	37.963	37.963
M=40	37.972	37.953	<b>37.962</b>	<b>37.962</b>	<b>37.962</b>	<b>37.962</b>	<b>37.962</b>	<b>37.962</b>	<b>37.962</b>	<b>37.962</b>	<b>37.962</b>	<b>37.962</b>
M=60	37.965	37.958	<b>37.962</b>	<b>37.962</b>	<b>37.962</b>	<b>37.962</b>	<b>37.962</b>	<b>37.962</b>	<b>37.962</b>	<b>37.962</b>	<b>37.962</b>	<b>37.962</b>
M=80	37.962	37.960	<b>37.962</b>	<b>37.962</b>	<b>37.962</b>	<b>37.962</b>	<b>37.962</b>	<b>37.962</b>	<b>37.962</b>	<b>37.962</b>	<b>37.962</b>	<b>37.962</b>
M=100	37.961	37.960	<b>37.962</b>	<b>37.962</b>	<b>37.962</b>	<b>37.962</b>	<b>37.962</b>	<b>37.962</b>	<b>37.962</b>	<b>37.962</b>	<b>37.962</b>	<b>37.962</b>
m=1, n=1; IV mode												
	N=1	N=2	N=3	N=4	N=5	N=6	N=7	N=8	N=9	N=10	N=11	N=12
M=5	46.010	421.88	NaN	NaN	44.746	44.590	44.576	44.594	44.643	44.593	55.818	44.593
M=10	435.65	NaN	42.865	41.753	510.89	65.792	44.443	44.597	44.597	44.597	44.597	44.597
M=20	9932.8	44.529	44.593	44.593	44.593	44.593	44.593	44.593	44.593	44.593	44.593	44.593
M=40	44.607	44.576	44.592	44.592	44.592	44.592	44.592	44.592	44.592	44.592	44.592	44.592
M=60	44.594	44.584	44.592	44.592	44.592	44.592	44.592	44.592	44.592	44.592	44.592	44.592
M=80	44.591	44.588	44.592	44.591	44.592	44.592	44.592	44.592	44.592	44.592	44.592	44.592
M=100	44.590	44.590	44.589	44.592	<b>44.591</b>	<b>44.591</b>	<b>44.591</b>	<b>44.591</b>	<b>44.591</b>	<b>44.591</b>	<b>44.591</b>	<b>44.591</b>

Table 12: Sandwich spherical shell with composite skins and thickness ratio  $R_\alpha/h=5$ . Modes from I to IV ( $m=n=1$ ) given as dimensionless circular frequency  $\bar{\omega} = \omega(a^2/h)\sqrt{\rho_{skin}/E_{2skin}}$ . Five physical layers ( $N_L=5$ ) divided in M mathematical layers.

Mode	(m,n)	I	II	III
$0^\circ/90^\circ$				
Present 3D	(1,1)	0.060274	0.52994	0.58275
3D [18]	(1,1)	0.060274	0.52994	0.58275
Present 3D	(1,2)	0.14538	0.62352	0.95652
3D [18]	(1,2)	0.14539	0.62352	0.95652
Present 3D	(2,1)	0.14538	0.62352	0.95652
3D [18]	(2,1)	0.14539	0.62352	0.95652
Present 3D	(2,2)	0.20229	0.95796	1.0300
3D [18]	(2,2)	0.20229	0.95796	1.0300
$0^\circ/90^\circ/0^\circ$				
Present 3D	(1,1)	0.067147	0.50349	0.63775
3D [18]	(1,1)	0.067147	0.50349	0.63775
Present 3D	(1,2)	0.12811	0.6888	0.95017
3D [18]	(1,2)	0.12811	0.6888	0.95017
Present 3D	(2,1)	0.17217	0.58366	1.1780
3D [18]	(2,1)	0.17217	0.58366	1.1780
Present 3D	(2,2)	0.20798	0.97517	1.2034
3D [18]	(2,2)	0.20798	0.97517	1.2034
$0^\circ/90^\circ/0^\circ/90^\circ$				
Present 3D	(1,1)	0.066210	0.54596	0.59995
3D [18]	(1,1)	0.066210	0.54596	0.59996
Present 3D	(1,2)	0.15194	0.63875	1.0761
3D [18]	(1,2)	0.15194	0.63875	1.0761
Present 3D	(2,1)	0.15194	0.63875	1.0761
3D [18]	(2,1)	0.15194	0.63875	1.0761
Present 3D	(2,2)	0.20841	1.0623	1.1557
3D [18]	(2,2)	0.20841	1.0623	1.1557

Table 13: Assessment for a simply supported multilayered composite square plate ( $a/h=10$ ). First three exact natural circular frequencies in dimensionless form  $\bar{\omega} = \omega h \sqrt{\frac{\rho}{E_2}}$  for imposed half-wave numbers (m,n). Comparison between the present three-dimensional analysis (M=2, 3, 4 and N=12) and the three-dimensional analysis by Messina [18].

m,n	mode	$N_L=2$		$N_L=4$		$N_L=10$	
		Present 3D	3D [23]	Present 3D	3D [23]	Present 3D	3D [23]
1,1	I	1.8971	1.8971	2.3415	2.3415	2.4930	2.4930
1,1	II	18.813	18.813	21.545	21.545	22.387	22.387
1,1	III	20.169	20.169	22.902	22.902	23.694	23.694
1,2	I	4.4492	4.4492	4.9620	4.9620	5.3017	5.3017
1,3	I	7.8195	7.8195	8.0753	8.0752	8.5253	8.5254
2,1	I	4.3485	4.3485	4.8493	4.8493	5.1853	5.1853
2,2	I	6.0384	6.0384	6.5486	6.5486	6.9739	6.9739
2,3	I	8.8895	8.8895	9.1438	9.1438	9.6346	9.6347
3,1	I	7.7503	7.7503	7.9573	7.9573	8.3950	8.3952
3,2	I	8.9012	8.9012	9.1290	9.1290	9.6120	9.6122
3,3	I	11.103	11.103	11.164	11.164	11.686	11.686

Table 14: Assessment for a simply supported multilayered composite cylindrical shell panel ( $R_\alpha/h=20$ ). Modes versus half-wave numbers (m,n) for several physical layers ( $N_L$ ) and lamination sequence ( $0^\circ/90^\circ/0^\circ/90^\circ/\dots$ ). Comparison between the present three-dimensional analysis ( $M=100$  and  $N=3$ ) and the three-dimensional analysis by Huang [23] in term of dimensionless circular frequencies  $\bar{\omega} = \omega R_\alpha \sqrt{\frac{\rho}{E_0}}$ .

m,n	mode	$N_L=2$		$N_L=4$		$N_L=10$	
		Present 3D	3D [23]	Present 3D	3D [23]	Present 3D	3D [23]
1,1	I	4.6240	4.6238	5.8070	5.8070	6.2293	6.2293
1,2	I	10.753	10.753	12.134	12.134	13.050	13.050
1,3	I	19.130	19.130	19.845	19.846	21.042	21.042
2,1	I	10.864	10.864	12.188	12.188	13.076	13.076
2,2	I	14.909	14.909	16.298	16.298	17.432	17.432
2,3	I	21.961	21.961	22.719	22.719	24.027	24.027
3,1	I	19.315	19.315	19.931	19.932	21.081	21.082
3,2	I	22.053	22.053	22.757	22.757	24.045	24.045
3,3	I	27.483	27.483	27.790	27.790	29.189	29.189

Table 15: Assessment for a simply supported multilayered composite spherical shell panel ( $R_\alpha/h=50$ ). Modes versus half-wave numbers (m,n) for several physical layers ( $N_L$ ) and lamination sequence ( $0^\circ/90^\circ/0^\circ/90^\circ/\dots$ ). Comparison between the present three-dimensional analysis ( $M=100$  and  $N=3$ ) and the three-dimensional analysis by Huang [23] in term of dimensionless circular frequencies  $\bar{\omega} = \omega R_\alpha \sqrt{\frac{\rho}{E_0}}$ .

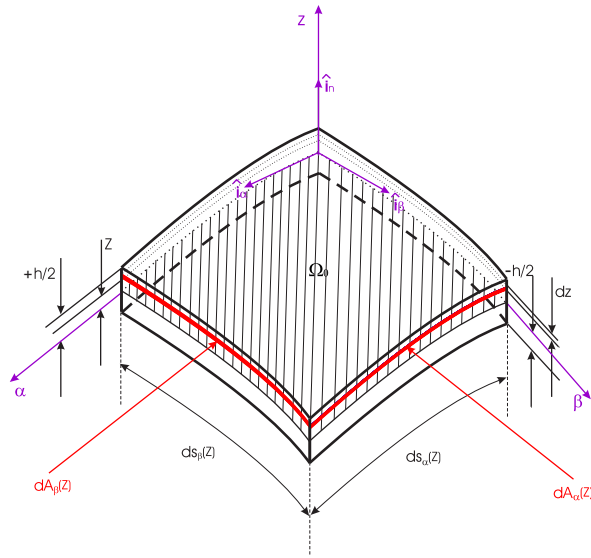


Figure 1: Notations, reference system and geometrical parameters for shell structures.

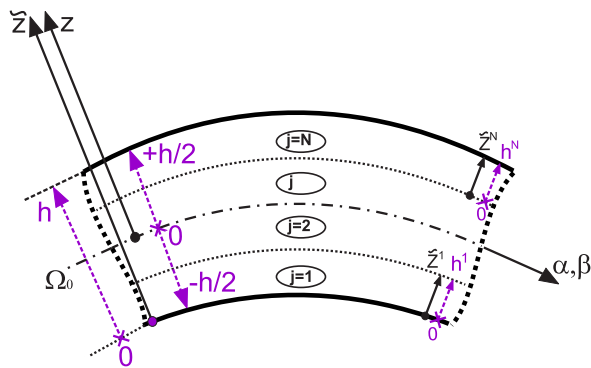


Figure 2: Thickness coordinates  $z$  and  $\tilde{z}$ , and reference systems for shell structures.

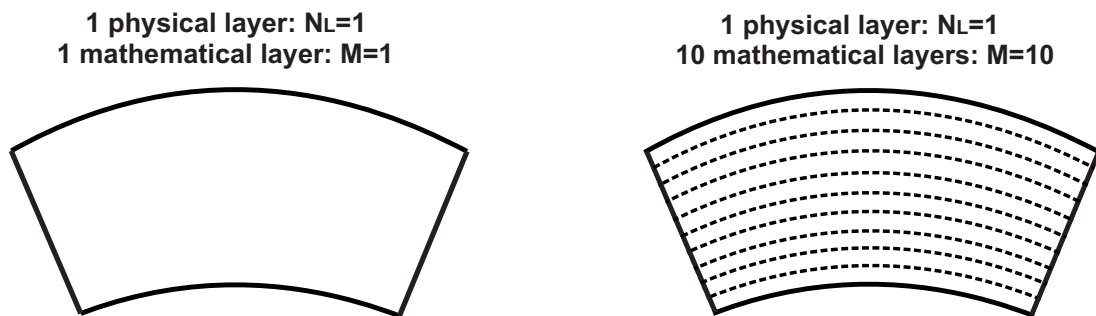


Figure 3: One-layered structures, example for the use of  $M$  mathematical layers.

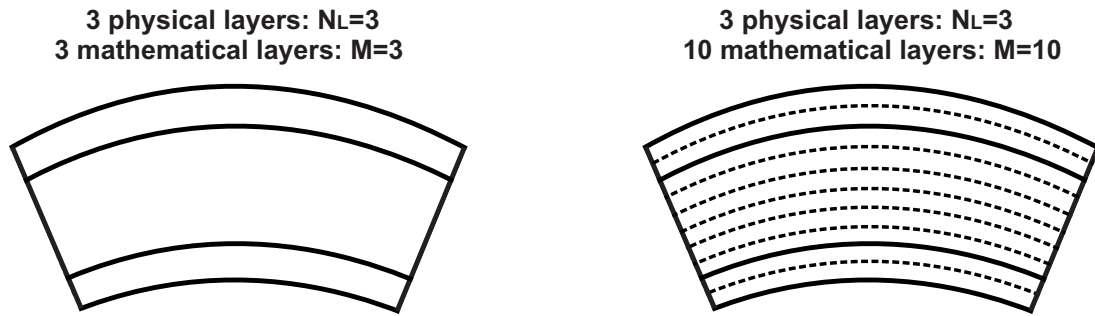


Figure 4: Three-layered sandwich structures, example for the use of  $M$  mathematical layers.

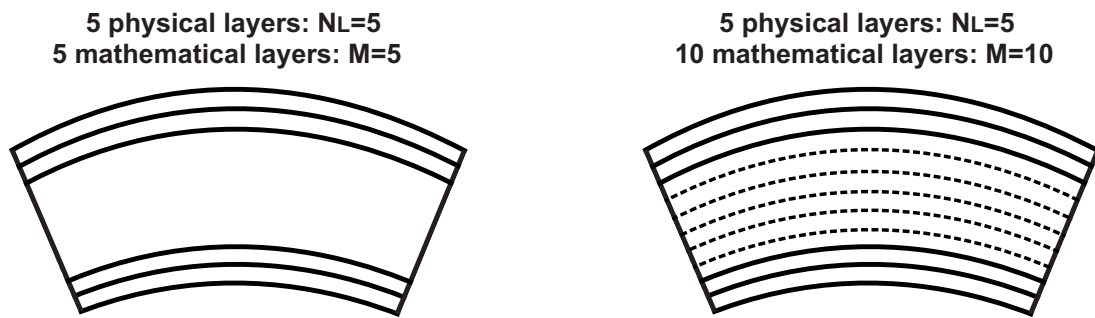


Figure 5: Five-layered sandwich structures, example for the use of  $M$  mathematical layers.

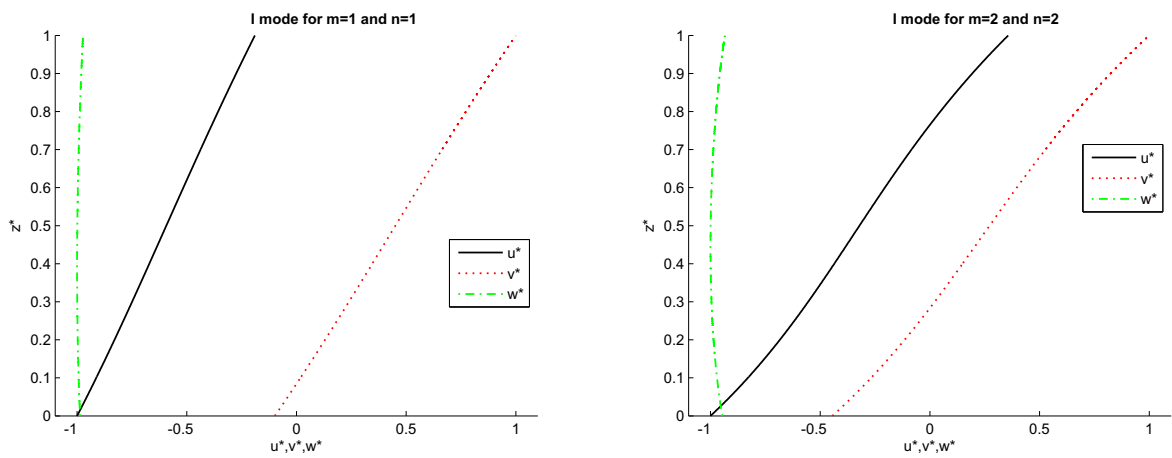


Figure 6: First mode (I) for one-layered isotropic cylindrical shell with  $R_\alpha/h=5$ .



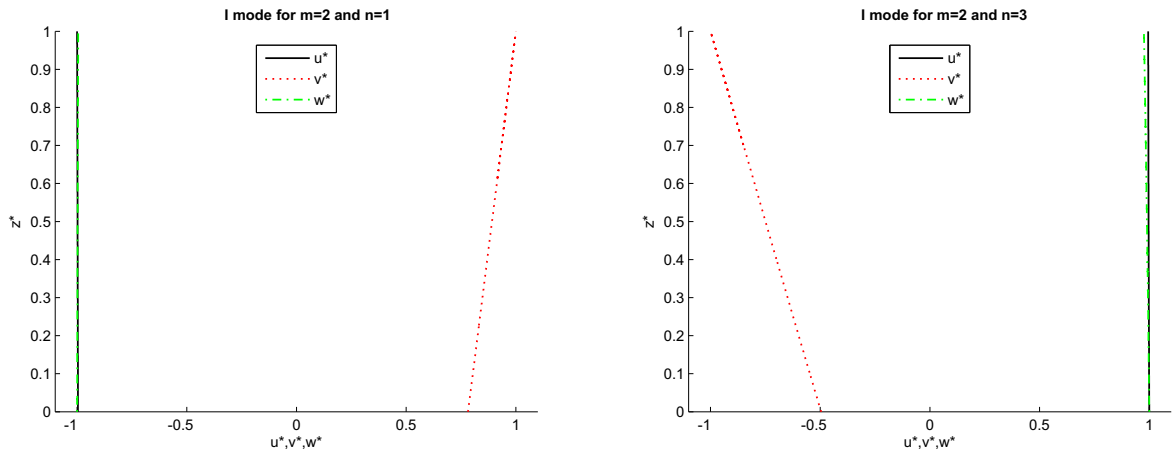


Figure 7: First mode (I) for one-layered isotropic cylinder with  $R_\alpha/h=5$ .

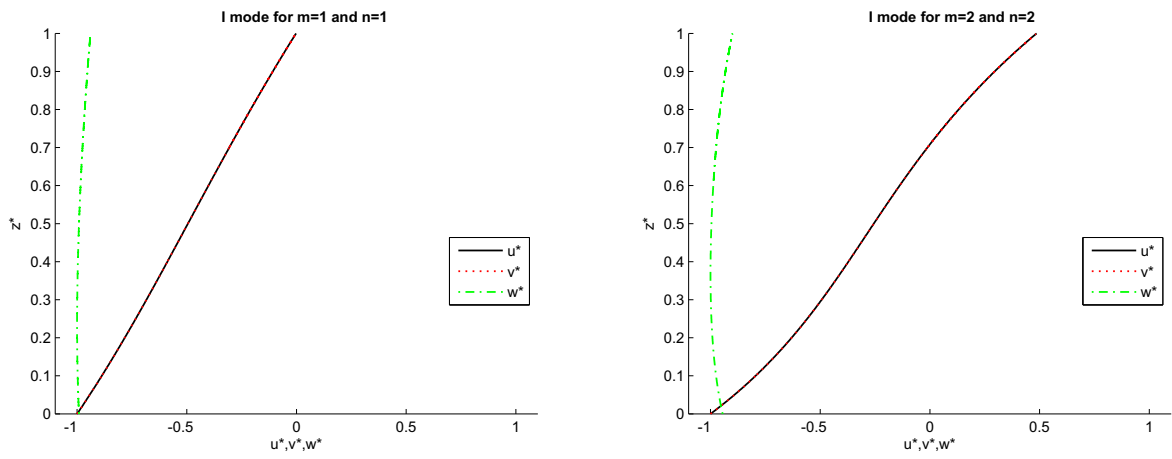


Figure 8: First mode (I) for one-layered isotropic spherical shell with  $R_\alpha/h=5$ .

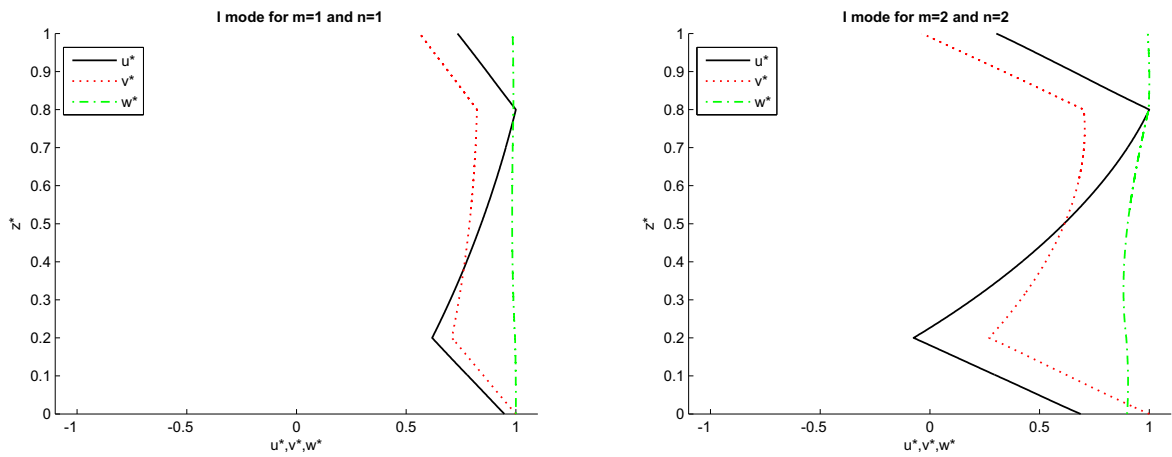


Figure 9: First mode (I) for sandwich spherical shell embedding composite skins with  $R_\alpha/h=5$ .

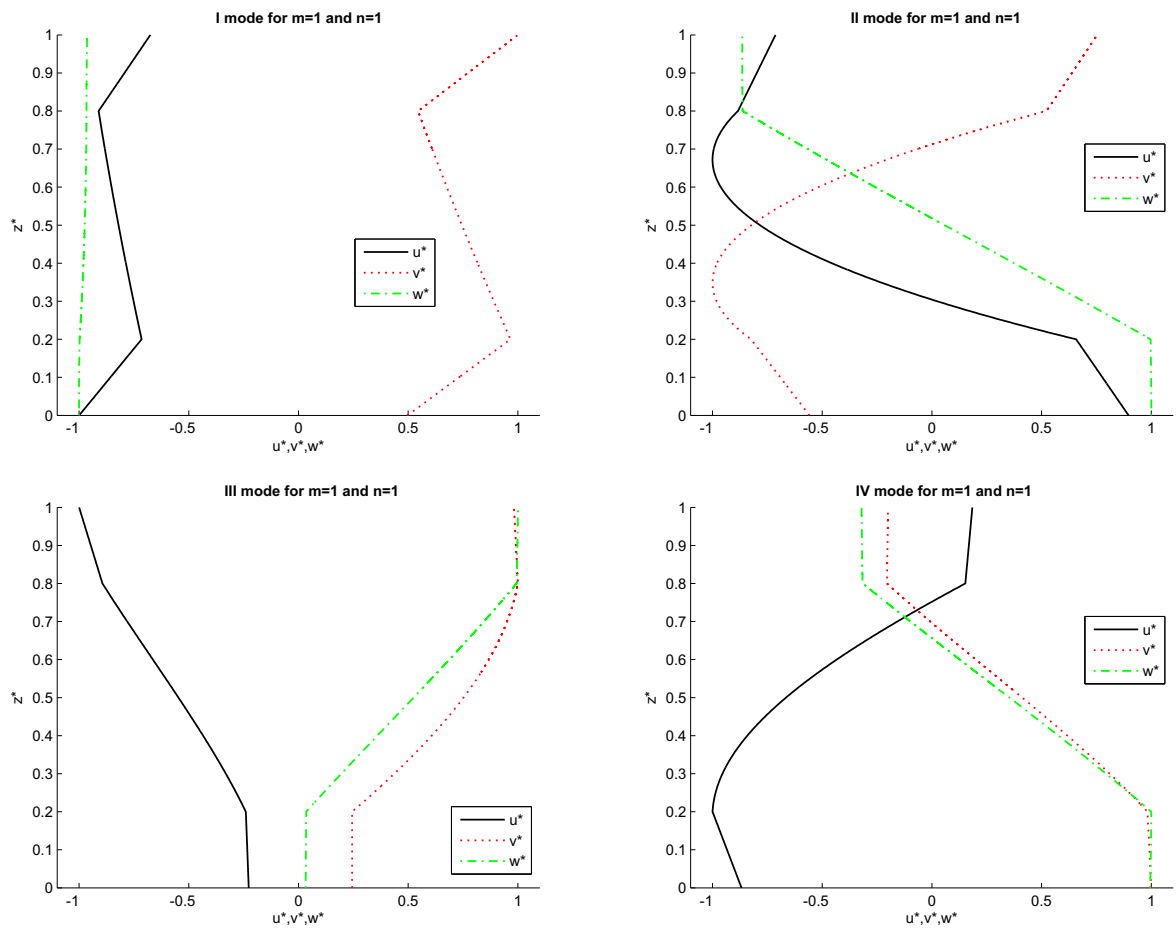


Figure 10: First four modes (I-IV) for sandwich cylindrical shell with isotropic skins and thickness ratio  $R_\alpha/h=5$ .

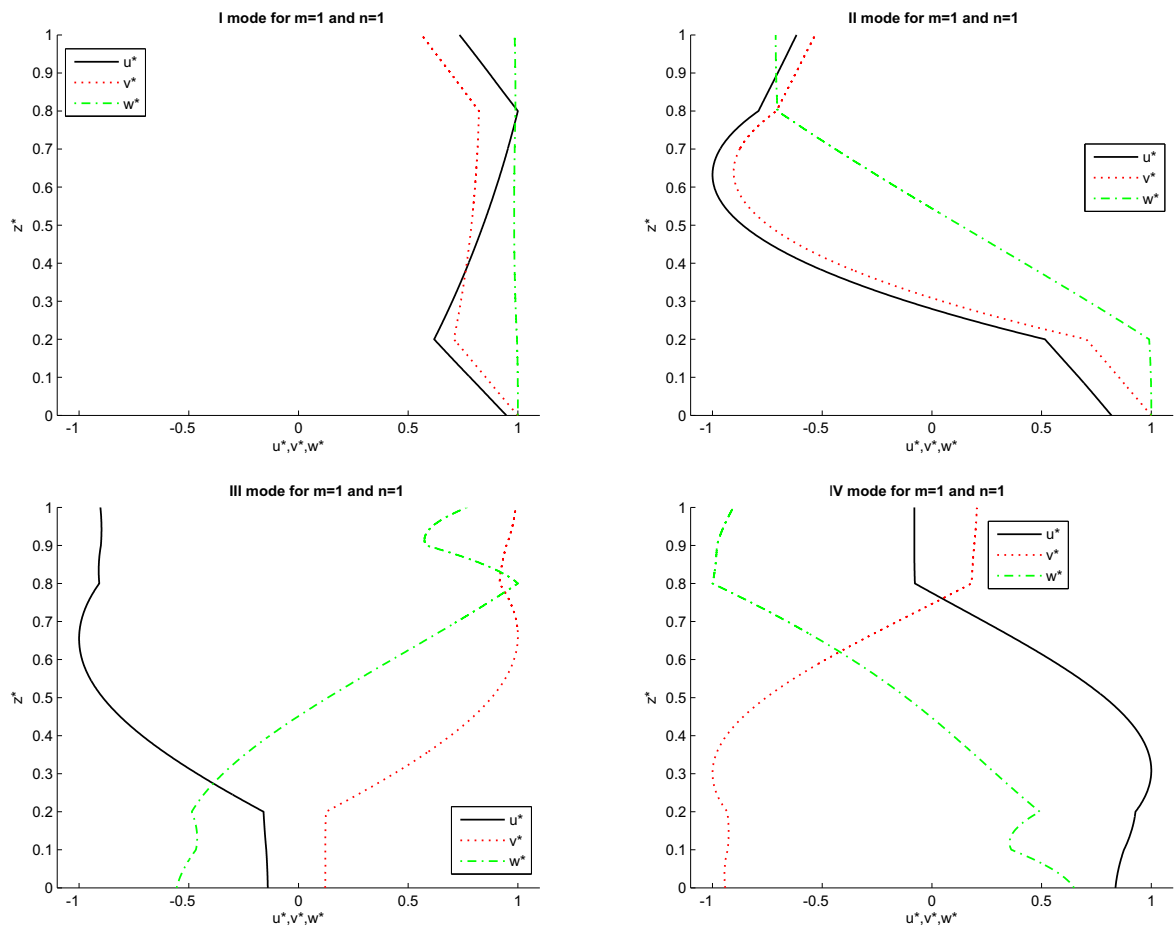


Figure 11: First four modes (I-IV) for sandwich spherical shell with composite skins and thickness ratio  $R_\alpha/h=5$ .